

**US Department of Energy  
FreedomCAR and Vehicle Technology Office**

**Innovative Structural and Joining Concepts for  
Lightweight Design of Heavy Vehicle Systems**

**Contract No. NT42476**

**FINAL REPORT**

**Jacky C. Prucz, Ph.D.  
Samir N. Shoukry, Ph.D.  
Gergis W. William, Ph.D., P.E.  
Thomas H. Evans, MSME**

**Department of Mechanical and Aerospace Engineering  
College of Engineering and Mineral Resources**

**West Virginia University**

**September 2006**

## DISCLAIMER

This report was prepared as an account of work sponsored by an agency of the United States Government. Neither the United States Government nor any agency thereof, nor any of their employees, makes any warranty, express or implied, or assumes any legal liability or responsibility for the accuracy, completeness, or usefulness of any information, apparatus, product, or process disclosed, or represents that its use would not infringe privately owned rights. Reference herein to any specific commercial product, process, or service by trade name, trademark, manufacturer, or otherwise does not necessarily constitute or imply its endorsement, recommendation, or favoring by the United States Government or any agency thereof. The views and opinions of authors expressed herein do not necessarily state or reflect those of the United States Government or any agency thereof.

## TABLE OF CONTENTS

TABLE OF CONTENTS	ii
LIST OF FIGURES	iv
LIST OF TABLES	vii
CHAPTER ONE	
<b>INTRODUCTION</b>	1
1.1 Background	1
1.2 Objectives	2
CHAPTER TWO	
<b>DEVELOPMENT AND VALIDATION OF INTEGRATED DESIGN CONCEPTS</b>	3
2.1 Introduction	3
2.2 Modeling of Trailer Floor	4
CHAPTER THREE	
<b>ANALYSIS OF VARIOUS CROSS SECTIONS FOR THE CORE STRUCTURE OF EXTRUDED SUPPORT MEMBERS</b>	9
3.1 Introduction	9
3.2 Cross Sections	9
3.3 Bending Analysis	10
3.3.1 Bending Results	11
3.3.2 Discussion of Finite Element Bending Results	17
3.4 Torsion Analysis	17
3.5 Comparison of Bending and Torsion Results	25
3.6 Weight Comparison	26
CHAPTER FOUR	
<b>PROTOTYPING AND TESTING OF LIGHTWEIGHT STRUCTURAL ASSEMBLIES</b>	29
4.1 Innovative Structural Joining Configurations	29
4.1.1 Development of Model Joints and Prototype Design	29
4.2 Prototyping of Innovative Structural and Joining Concepts	33
4.2.1 Manufacturing Process	33
4.2.2 Trailer Model	34
4.2.3 Modular Design	36
4.3 Panels with Tube Section Cross Members	37
4.4 Testing of Sandwich Panel Prototypes	39
4.5 Finite Element Analysis (ANSYS)	46
4.6 Failure Analysis	53
4.7 Discussion	58
CHAPTER FIVE	
<b>IMPACT AND FLEXURAL TESTING ON SANDWICH PANELS</b>	64

5.1	Introduction	64
5.2	Impact Testing	64
5.3	Future Panel Configurations	67
5.4	Flexural Testing	68
CHAPTER SIX		
	<b>CONCLUSIONS</b>	73
	<b>FY 2005 PUBLICATIONS/PRESENTATIONS</b>	74
	<b>REFERENCES</b>	75

## LIST OF FIGURES

Figure 2.1	A Schematic Showing the Dimensions of the Floor Configurations Considered in the Study. The length of the full floor is 48', whereas its width is 8'.	4
Figure 2.2	Three-Dimensional Finite Element Models for Floor Design Configurations	5
Figure 2.3	Finite Element Model of the Full Floor of The Trailer, As Displayed With Boundary Conditions	6
Figure 2.4	Contours of Transverse Displacements for 4 Floor Designs.	7
Figure 3.1	The Six Different Cross Sections of the Core Structure	9
Figure 3.2	Representation of a Sandwich Composite Structure Using the X2 Core Cross Section	10
Figure 3.3	Loading Scenario, Dimensions, and Boundary Conditions for Bending Analysis	10
Figure 3.4	Tube Displacement Using ANSYS	11
Figure 3.5	Slant Displacement Using ANSYS	12
Figure 3.6	X1 Displacement Using ANSYS	12
Figure 3.7	X2 Displacement Using ANSYS	13
Figure 3.8	Box Displacement Using ANSYS	13
Figure 3.9	Box2 Displacement Using ANSYS	14
Figure 3.10	Tube Displacement Using ADINA	14
Figure 3.11	Slant Displacement Using ADINA	15
Figure 3.12	X1 Displacement Using ADINA	15
Figure 3.13	X2 Displacement Using ADINA	15
Figure 3.14	Box Displacement Using ADINA	16
Figure 3.15	Box2 Displacement Using ADINA	16
Figure 3.16	Loading Scenario, Dimensions and Boundary Conditions for Torsional Analysis	17
Figure 3.17	Tube Torsion Results Using ANSYS	18
Figure 3.18	Slant Torsion Results Using ANSYS	19
Figure 3.19	X1 Torsion Results Using ANSYS	19
Figure 3.20	X2 Torsion Results Using ANSYS	20
Figure 3.21	Box Torsion Results Using ANSYS	20
Figure 3.22	Box2 Torsion Results Using ANSYS	21
Figure 3.23	Tube Torsion Results Using ADINA	22
Figure 3.24	Slant Torsion Results Using ADINA	22
Figure 3.25	X1 Torsion Results Using ADINA	23
Figure 3.26	X2 Torsion Results Using ADINA	23
Figure 3.27	Box Torsion Results Using ADINA	24
Figure 3.28	Box2 Torsion Results Using ADINA	24
Figure 3.29	Plot of Maximum Bending Deflection for Tube Cross Members	25
Figure 3.30	Plot of Maximum Torsional Stress within the Tube Cross Members	26
Figure 3.31	Plot of the Weight Comparison between Cross Tube Members	27
Figure 4.1	Alternative Design Concepts for the Floor Platform of a Modified Van Trailer	29
Figure 4.2	Sandwich Composite Structure with Aluminum Tube Core Construction for Flooring Platform Applications. Design concept C	30
Figure 4.3	Type D Flooring Alternative Using Composite I-Beams as Cross Member Supports and Composite Bearing Bars	30
Figure 4.4	Connection Method between Side Panels by an H-Joint Configuration	31
Figure 4.5	Double Corner Joint	31
Figure 4.6	Corner Joint for Connecting the Floor Platform to the Sidewall or Side Panels of a Van Trailer	32

Figure 4.7	Alternative Option for the Corner Joint Connecting the Side Panels to the Flooring Platform	32
Figure 4.8	Scaled Prototype of the Replica 1:4 Trailer Model Emphasizing the Locations and Types of Joints	35
Figure 4.9	Unassembled Sections of the Model Trailer	35
Figure 4.10	Method of Joining the Segments of the Van Trailer by Connecting the I-Beam Cross Members	36
Figure 4.11	A Method to Assist the Joining of Segments for the Modular Application of the Van Trailer Design	36
Figure 4.12	Load vs. Strain Plots of the <i>Tubeplate</i> Experiment Test	39
Figure 4.13	Shearing Strain Values for the <i>Tuneplate</i> Configuration at the Inset of the Supported Edges	40
Figure 4.14	Load vs. Strain Plots of the <i>Tubegrate</i> Experiment Test	41
Figure 4.15	Shearing Strain Values for the <i>Tunegrate</i> Configuration at the Inset of the Supported U-Channel Edges	42
Figure 4.16	Load vs. Strain Plots of the <i>Fiberplate</i> Experimental Test	43
Figure 4.17	Shear Strain Values for the <i>Fiberplate</i> Configuration at the Inset of the Simply Supported Edges	44
Figure 4.18	Load vs. Strain Plots of the <i>Carbonplate</i> Experimental Test	45
Figure 4.19	Shear Strain Values for the <i>Carbonplate</i> Panel at the Inset of the Simply Supported Edges	46
Figure 4.20	Tubeplate Finite Element Model Displaying the Boundary Conditions, Load, and Coupled Degrees of Freedom as Weld Connections	47
Figure 4.21	Strain in the Uniaxial Direction Corresponding to the Strain Gage Placement in the Experimental Analysis	48
Figure 4.22	Magnified View of the Uniaxial Strain Next to the Load Area. Notice the Stress Concentration Next to the Weld Point	48
Figure 4.23	Tubegrate Finite Element Model Showing the Contact Load, Edge Restraints, and Coincident Nodes	49
Figure 4.24	Uniaxial Strain of The Tubegrate Panel	50
Figure 4.25	The <i>Fiberplate</i> Finite Element Model Showing the Simply Supported Edges and Load	51
Figure 4.26	Uniaxial and Shear Strains of the <i>Fiberplate</i> Panel	51
Figure 4.27	Uniaxial and Shear Strains of the <i>Carbonplate</i> Panel	53
Figure 4.28	Contour Plot of Von-Mises Stress in the Fiberplate	54
Figure 4.29	Contour Plot of the Von-Mises Stress in the Core of the Fiberplate	54
Figure 4.30	Contour Plot of Von-Mises Stress in the Carbonplate	55
Figure 4.31	Contour Plot of the Von-Mises Stress in the Core of the Carbonplate	55
Figure 4.32	Finite Element Models of the Trailer Section and the Carbonplate	59
Figure 4.33	Displacement Contour Plot of the Trailer Section Model	59
Figure 4.34	Displacement Contour Plot of the Carbonplate-4 Section	60
Figure 4.35	Shear Strain Contour Plot of the Trailer Section Model	60
Figure 4.36	Shear Strain Contour Plot of the Carbonplate-4 Model	61
Figure 4.37	Displacement Contour Plot of the Fiberglass-4 Section	62
Figure 4.38	Shear Strain Contour Plot of the Fiberglass-4 Model	62
Figure 5.1	Failure Modes under Different Bullet Impacts	66
Figure 5.2	Specimen Configuration with Kevlar/Epoxy Core	67
Figure 5.3	Three-Point Bending Testing Setup	68
Figure 5.4	Load-Displacement Relation for Aluminum and Epoxy Sandwich Panel	69
Figure 5.5	Load-Displacement Relation for 20 Gage Steel and Epoxy Sandwich Panel	69

Figure 5.6	Load-Displacement Relation for Steel and Epoxy Sandwich Panel of Different face sheet Thickness	70
Figure 5.7	Results of Three-Point Bending Tests on Sandwich Panels	71

## LIST OF TABLES

Table 2.1	Energy Savings Through Lightweight Floor Design and Joining Concepts	3
Table 2.2	Maximum Calculated Deflections	6
Table 3.1	ANSYS Bending Results	11
Table 3.2	ADINA Bending Results	16
Table 3.3	ANSYS Torsion Results	21
Table 3.4	ADINA Torsion Results	24
Table 3.5	Comparison of ANSYS and ADINA Bending and Torsion Results	25
Table 3.6	Weight Comparisons between Alternative Cross-Sections	28
Table 4.1	Configurations of Sandwich Panel Prototypes	38
Table 4.2	Failure Criteria for the <i>Fiberplate</i> and <i>Carbonplate</i> Core Structure	56
Table 4.3	<i>Fiberplate</i> Maximum Stress Criterion	57
Table 4.4	<i>Carbonplate</i> Maximum Stress Criterion	57
Table 4.5	Weight of Panel Designs Compared to an Existing Trailer Section	58
Table 5.1	Specimen Lay-up Configuration	64
Table 5.2	Specifications of Firearm and Bullet Weights	65
Table 5.3	Specifications of Rifles and Cartridges	65
Table 5.4	Data for Test Parameters	66
Table 5.5	Specimen Lay-up Configuration	68
Table 5.6	Specimen Lay-up Configuration	72



## CHAPTER ONE

### INTRODUCTION

#### 1.1 Background

The extensive research and development effort was initiated by the U.S. Department of Energy (DOE) in 2002 at West Virginia University (WVU) in order to investigate practical ways of reducing the structural weight and increasing the durability of heavy vehicles through the judicious use of lightweight composite materials. While this project was initially focused on specific Metal Matrix Composite (MMC) material, namely Aluminum/Silicon Carbide (Al/SiC) commercially referenced as “LANXIDE”, the current research effort was expanded from the component level to the system level and from MMC to other composite material systems. Broadening the scope of this research is warranted not only by the structural and economical deficiencies of the “LANXIDE” MMC material, but also by the strong coupling that exists between the material and the geometric characteristics of the structure. Such coupling requires a truly integrated design approach, focused on the heaviest sections of a van trailer. Obviously, the lightweight design methods developed in this study will not be implemented by the commercial industry unless the weight savings are indeed impressive and proven to be economically beneficial in the context of Life Cycle Costs (LCC). “Bulk Haul” carriers run their vehicles at maximum certified weight, so that each pound saved in structural weight would translate into additional pound of cargo, and fewer vehicles necessary to transport a given amount of freight. It is reasonable to ascertain that a typical operator would be ready to pay a premium of about \$3-4 for every additional pound of cargo, or every pound saved in structural weight.

The overall scope of this project is to devise innovative, lightweight design and joining concepts for heavy vehicle structures, including cost effective applications of components made of metal matrix composite (MMC) and other composite materials in selected sections of such systems. The major findings generated by this research effort in its first two years have been summarized in the 2003 and 2004 Annual Progress Reports of DOE’s Freedom Car and Vehicle Technologies Program (*Prucz and Shoukry 2004; Prucz et al., 2005*).

Consistent interactions with producers of heavy trailers, such as Great Dane and Wabash, as well as with their users, such as Old Dominion Freight Lines, have continued during this period to ensure that the research conducted at WVU will yield practical results that will benefit the industry in the near future. Furthermore, Dr. Gergis William and Mr. Thomas Evans participated in the 2005 Technology and Maintenance Council (TMC) annual meeting held in Tampa, Florida, in February 2005. This event offered the WVU researchers an effective opportunity to explore various technical needs and concerns of the industry, both from the performance and maintenance viewpoints, as well as to assess realistically potential benefits and barriers associated with practical implementation of lightweight materials and design technologies in heavy vehicle structures.

## 1.2 Objectives

The research work proposed in this study for the fiscal year FY2005 (April 1, 2005 through March 31, 2006) continues and validates the research work conducted in the past two years to develop innovative joining and design concepts for lightweight and durable structural systems for heavy vehicles (*Prucz et al., 2005 a, b, Prucz and Shoukry 2004*). Prototyping and testing facilities available at West Virginia University provides the basis for showcasing the new concepts to industry, in support of future commercial applications of the technology developed through this project. The collaboration with industrial partners, both from the trailer manufacturing and the freight line industries, is further enhanced for this purpose.

The research work proposed in this study is guided and assessed by achieving the following primary milestones:

- Comprehensive presentation on integrated development and validation of lightweight design configurations for the chassis and body structures of a typical van trailer.
- Showcasing of laboratory experiments in simulated operation scenarios of baseline and improved prototypes of typical trailer structures and components.
- Presentation on preliminary durability predictions for fiber reinforced composites and sandwich panels in floor structure of a heavy van trailer.


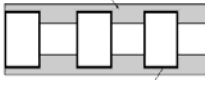
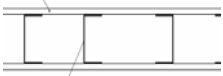
## CHAPTER TWO

### DEVELOPMENT AND VALIDATION OF INTEGRATED DESIGN CONCEPTS

#### 2.1 Introduction

A preliminary structural analysis was conducted in the past two years of the project. The results of this research effort indicated that the chassis assembly contributes currently about 73 percent of the overall weight of a typical van trailer (15,100 lb for a 48 ft long trailer). About 47 percent of the weight of the chassis is contributed by the oak floor panels and the cross beams that support the floor (*Prucz and Shoukry, 2004; Prucz et al., 2005*). Alternative design and joining concepts for the structural floor of a van trailer were devised as part of this project, in order to reduce its weight significantly below that of the current design configuration. All these lightweight designs rely on sandwich panels with various material and geometric characteristics of the core layer(s). The main objective of the new designs was to achieve optimal tradeoffs between the overall structural weight and the flexural stiffness of the floor. The predicted energy savings enabled by the lightweight floor design and joining configurations of a typical van trailer are shown in Table 2.1. Although these numbers appear to be small for transporting one ton of cargo, they become enormously significant considering the thousands and thousands of freight that any given trailer is likely to haul during its life in service.

Table 2.1 - Energy Saving Through Lightweight Floor Design and Joining Concepts.

Alternative lightweight designs, based on sandwich panel configurations, for the floor of a typical heavy van trailer	Minimum Weight (lb)	Weight Saving (%)	Gallons of Fuel Used to Transport One Ton of Cargo Over 1000 Miles
Current configuration	6980	0%	5.82 (0.0%)
Fiberglass cross-beams 	2802	60%	5.41 (7.0%)
Fiberglass Face-Plates, Core of Magnesium Hollow Tubes 	3701	47%	5.49 (5.7%)
Fiberglass Face-Plates, Core of Magnesium C-Channels 	3252	53%	5.45 (6.4%)
MMC Duralcan Face-Plates with lightweight core, such as Balsa	2964	57%	5.43 (6.7%)

Since the operators of long haul heavy trailers usually load them to reach the gross vehicle weight (GVW) in order to maximize the efficiency of every transport, structural weight

reductions would not necessarily result in lower fuel consumption of the truck in terms of “miles per gallon”. Instead, the associated energy savings are best expressed in terms of fuel used by a heavy vehicle to transport one ton of freight over a certain distance, say 1,000 miles [gal/(kip. mile)]. The comparison illustrated in Table 2.1 indicates that the current weight of the floor in a typical van trailer can be reduced to half, or even less, if a sandwich panel design configuration and joining concept devised at WVU is utilized. The figures presented in Table 2.1 are based on the floor and chassis assembly of a 48-ft long van trailer and a gross vehicle weight of 80 kips.

## 2.2 Modeling of Trailer Floor

Theoretical research efforts have continued on developing minimum weight design configurations for the chassis and floor of van trailers, which contribute about 73% of their overall structural weight. Three-dimensional finite element modeling and analysis was performed by using the ADINA commercial software package (*Bathe, 2002*) in order to compare the performance of four different candidate floor configurations for the design of lightweight van trailers.

The full span of the floor was modeled along with its major structural members such as cross-members and stiffeners. All cross-beam members of the floor were represented by using 8-node quadrilateral shell elements. Other major parts of the floor, namely the stiffeners, bogie I-beams and sidewalls were all represented by using beam elements. Four design configurations were modeled by using different cross-sectional shapes for the cross members, as those shown in Figure 2.1:

1. I-beams.
2. C- Channels.
3. Inverted U-Channels.
4. Z-Sections.

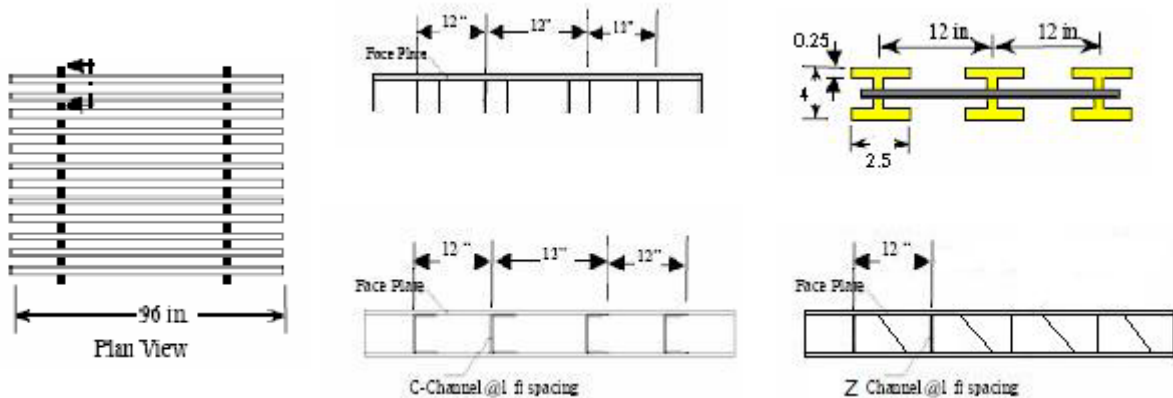


Figure 2.1 A Schematic Showing the Dimensions of the Floor Configurations Considered in the Study. The length of the full floor is 48', whereas its width is 8'

The following dimensions have been selected for the cross members in the above four design configurations: height = 4 inch, flange width = 2.5 inch, web thickness = 0.16 inch, and flange thickness = 0.25 inch. The floor thickness was assumed to be equal to be 0.75 inch. The finite element models developed for the four different design configurations are shown in Figure 2.2.

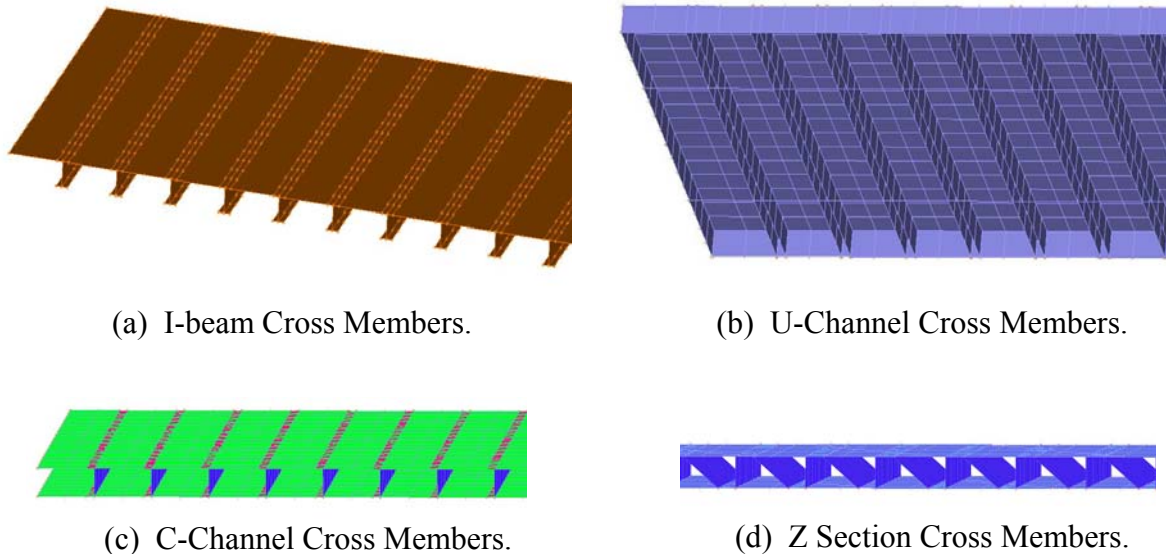


Figure 2.2 Three-Dimensional Finite Element Models for Floor Design Configurations.

The mesh sizes were adjusted in such a way that most of the nodes were common to two or more surfaces, thus reducing the need for contact elements. The length of the quad node was normally maintained at 6 inches. This approach resulted in models consisting of about 5,000 elements, on average. The cross-members were assumed to be made of steel (Modulus of Elasticity,  $E = 29$  Msi and Poisson's ratio,  $\nu=0.3$ ), while the top-covering layer of the floor is made of oak wood (Modulus of Elasticity,  $E = 1.6$  Msi and Poisson's ratio,  $\nu= 0.3$ ).

The boundary conditions of the models were formulated by assuming that the trailer was in stationary condition. The floor was constrained in the vertical, Z, direction at points where it rests on the landing gear and the bogie. Nodes corresponding to these locations were identified first, followed by applying the constraints directly on these nodes. Figure 2.3 shows the boundary conditions applied on the floor when looking up from below the floor. The points marked in green and magenta are the points where boundary conditions are applied.

Two types of loads, which typically act on a trailer while it is stationary, were considered in the analysis:

1. A static uniformly distributed transverse load that accounts for the payload

2. A static concentrated transverse load that accounts for the fork lift

The uniformly distributed load was applied as normal pressure acting on the top surface of the floor, and was calculated by assuming that the load-carrying capacity of the trailer is limited to 60,000 pounds. The four concentrated loads representing the four wheels of the forklift were calculated by assuming that each wheel carries a load of 10,000 pounds. The position of the concentrated loads is assumed to be at the center of the floor span, where the deflection is expected to be the highest. The structural behavior of each floor design configuration was determined and evaluated for the loading scenario where the above distributed and concentrated loads are superimposed.

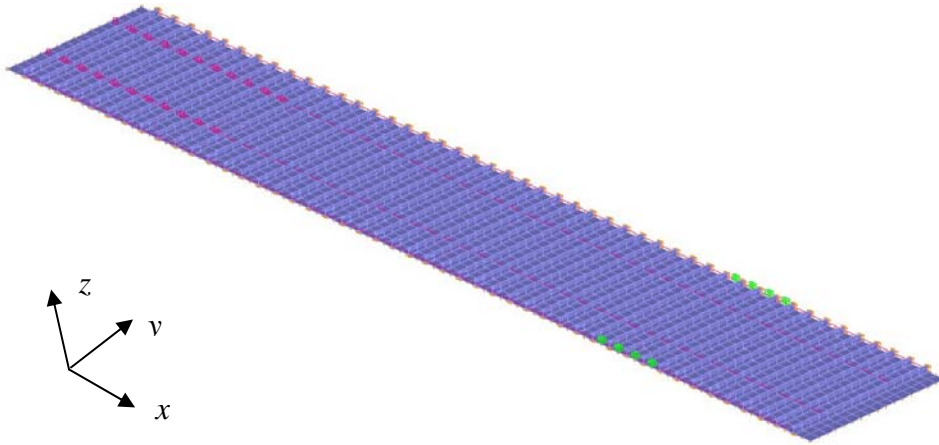
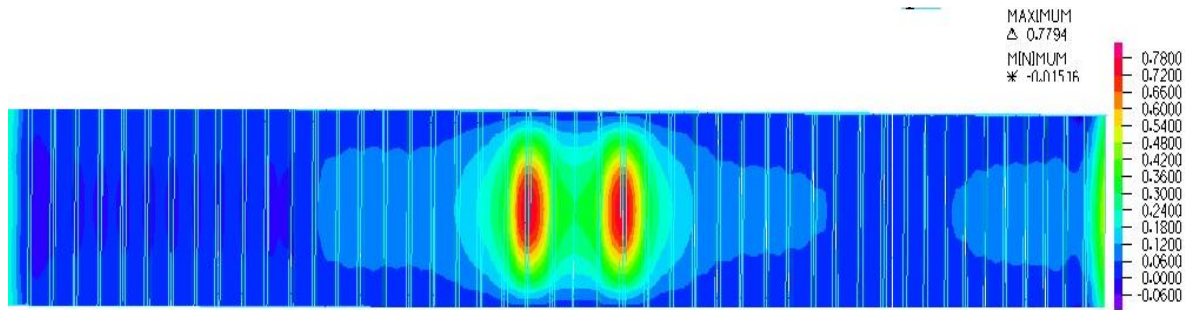


Figure 2.3 – Finite Element Model of the Full Floor of The Trailer, As Displayed With Boundary Conditions. The green points show the position of the landing gear and those marked in magenta show the points where the boogie meets the floor.

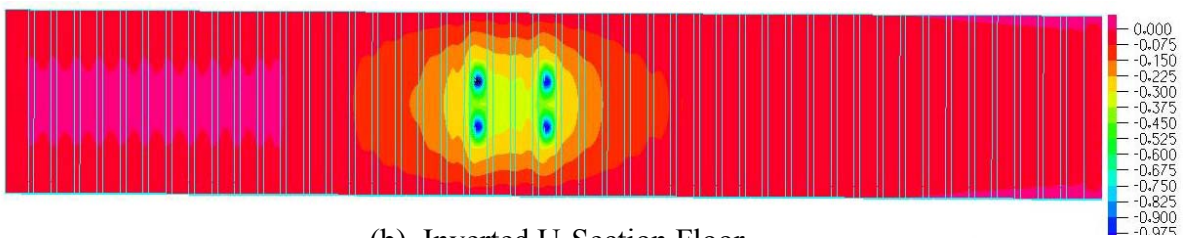
The performance parameter of interest in the structural response of the floor was its vertical displacement, in the z-direction, at the mid-span. The values calculated for this parameter for the above four types of trailer floors are compared in Table 2.2. It is worthy noticing that these results are highly sensitive to even small variations of geometric design parameters such as the width, spacing, or the thickness of cross-members. The data displayed in Table 2.2 indicate that the stiffest floor design is that based on cross members whose cross-section is in the shape of C-channel, whereas those whose cross-section is in the shape of an inverted U-section yield the design with the least stiffness. The displacement contours shown in Figure 2.4 confirm, indeed, the numerical results given in Table 2.2.

Table 2.2 Maximum Calculated Deflections.

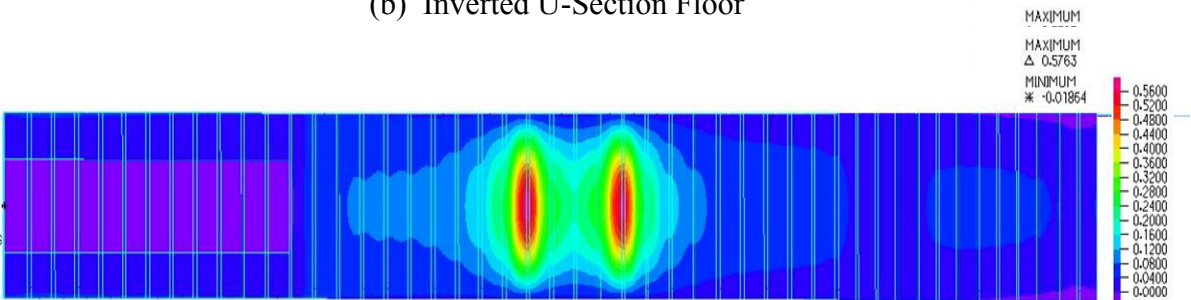
I-Section	0.779“
C-Section	0.575”
Inverted U-section	1.503”
Z-section	1.050”



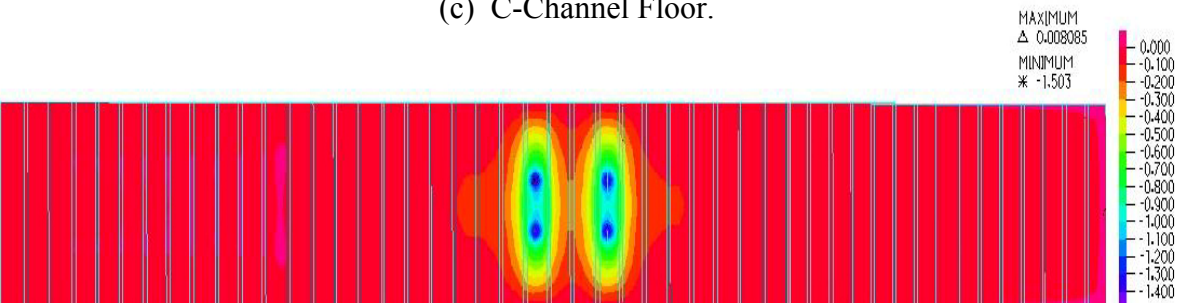
(a) Cross I-Beam Floor



(b) Inverted U-Section Floor



(c) C-Channel Floor.



(d) Z-Section Floor.

Figure 2.4 Contours of Transverse Displacements for 4 Floor Designs.

Though the trailer floor based on cross members with C-Sections appears to perform the best for displacement restrictions, it may not be the preferred configuration for reducing the overall weight of the floor. It is possible that one of other options, including the inverted U-

Sections exhibit, in fact, the design configuration with the lightest weight per unit area of the floor.



## CHAPTER THREE

### ANALYSIS OF VARIOUS CROSS SECTIONS FOR THE CORE STRUCTURE OF EXTRUDED SUPPORT MEMBERS

#### 3.1 Introduction

Various preliminary design concepts of the core material for the previously discussed Design III, or for the best option for trailer floor platform, were compared on the basis of a single section of the core structure. Six different designs were analyzed by weight, maximum displacement and maximum stress under bending and torsion loads. Each concept was kept uniform by length, thickness, loading and boundary conditions. Finite element modeling of the alternative structures was performed in both ANSYS and ADINA finite element programs.

#### 3.2 Cross Sections

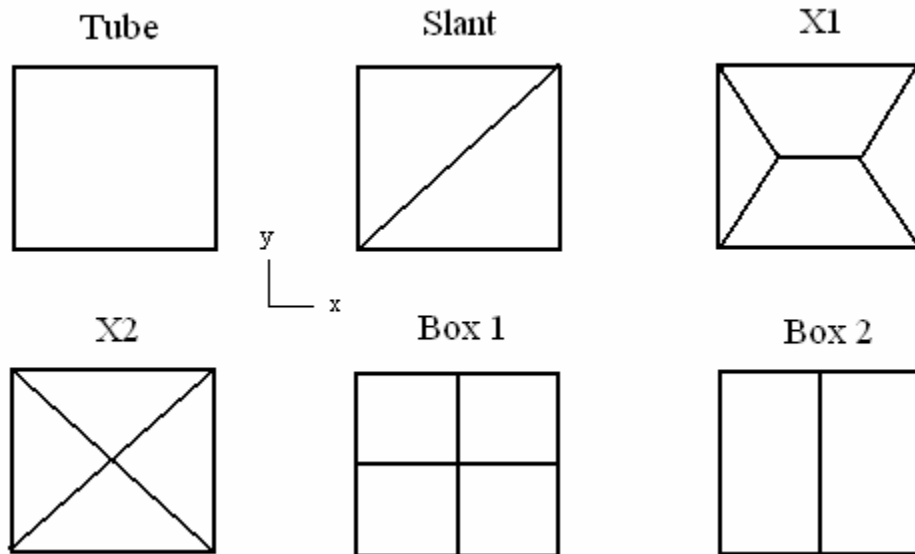


Figure 3.1 The Six Different Cross Sections of the Core Structure.

The cross sections being compared are shown in Figure 3.1. The cross sections represent a single part of the core structure of the flooring sandwich plate. Any of these sections will be repeated to form the core structure for the entire flooring platform. Figure 3.2 displays a possible flooring arrangement using, for example, the X2 section from Figure 3.1.

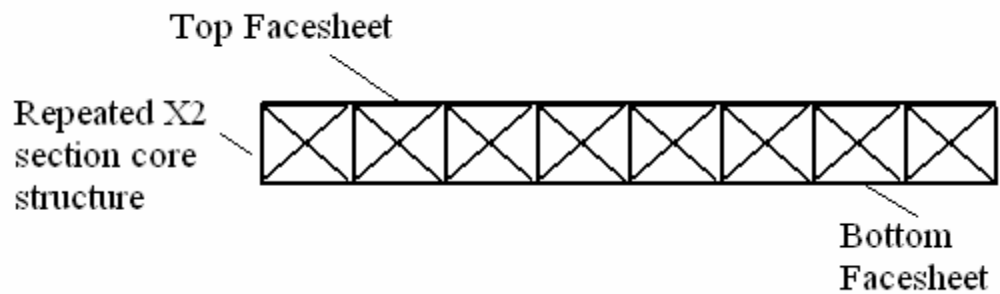


Figure 3.2 Representation of a Sandwich Composite Structure Using the X2 Core Cross Section.

Figure 3.2 shows how a single cross section will be repeated to build the core structure of the entire flooring. Therefore, to determine which arrangement is most beneficial, a finite element analysis and a weight analysis were performed. For accuracy and consistency, all loading, thicknesses, elements, element sizes, and boundary conditions were kept constant during the analysis of the different sections.

### 3.3 Bending Analysis

The parameters for the finite element bending analysis are given in this section. Referencing Figure 3.3, the load direction is in the negative  $y$  direction and has a value of 10 psi. This load is distributed over shell elements with dimensions of 0.5 in., 0.5 in., 0.02 in. in length, width, and thickness, respectively. The material properties correspond to standard aluminum with a Young's modulus value of  $26 \times 10^6$  psi and a Poisson's ratio of 0.33.

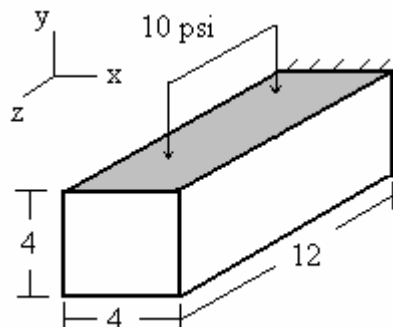


Figure 3.3 Loading Scenario, Dimensions, and Boundary Conditions for Bending Analysis.

Material: Aluminum  
 Elastic Modulus:  $26 \times 10^6$  psi  
 Poisson's ratio: 0.33  
 Loading: 10 psi in the negative  $y$  direction  
 Elements: Shell

Element size: 0.5 in.  
 Element thickness: 0.02 in.  
 Section Dimensions: 4 x 4 x 12 x 0.02 in.

### 3.3.1 Bending Results

The ANSYS generated results are displayed in Figures 3.4 to 3.9. The results display plots of maximum displacement distributions from an applied load of 10 psi. The corresponding numerical values of maximum displacements are summarized in Table 3.1.

Table 3.1 – ANSYS Bending Results

Cross Section	Maximum Displacement (in.)
Tube	0.997103
Slant	0.854074
X1	0.648361
X2	0.671524
Box 1	0.041566
Box 2	0.045573

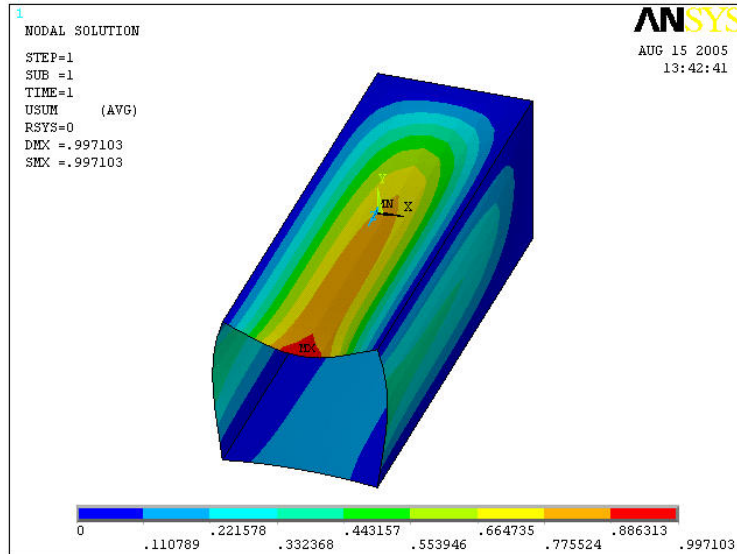


Figure 3.4 Tube Displacement Using ANSYS

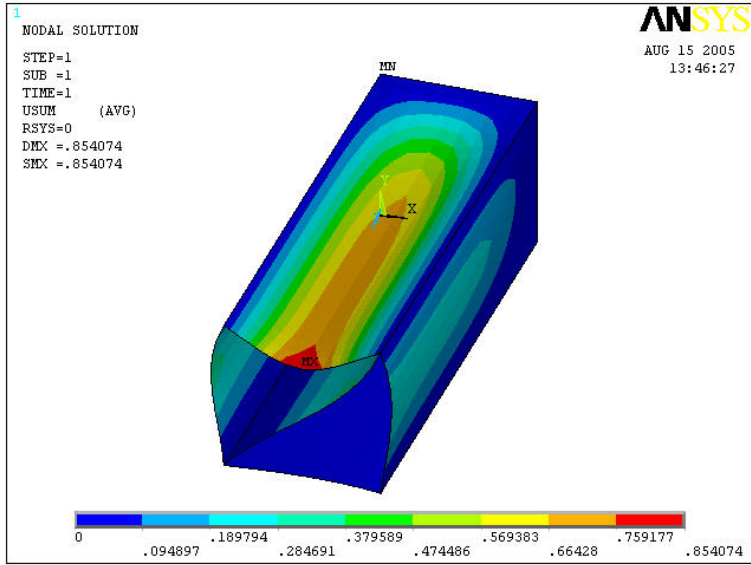


Figure 3.5 Slant Displacement Using ANSYS

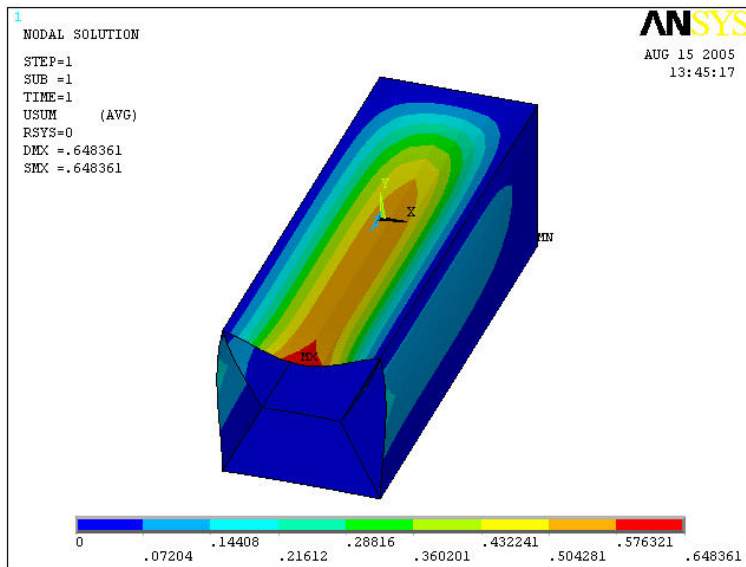


Figure 3.6 X1 Displacement Using ANSYS

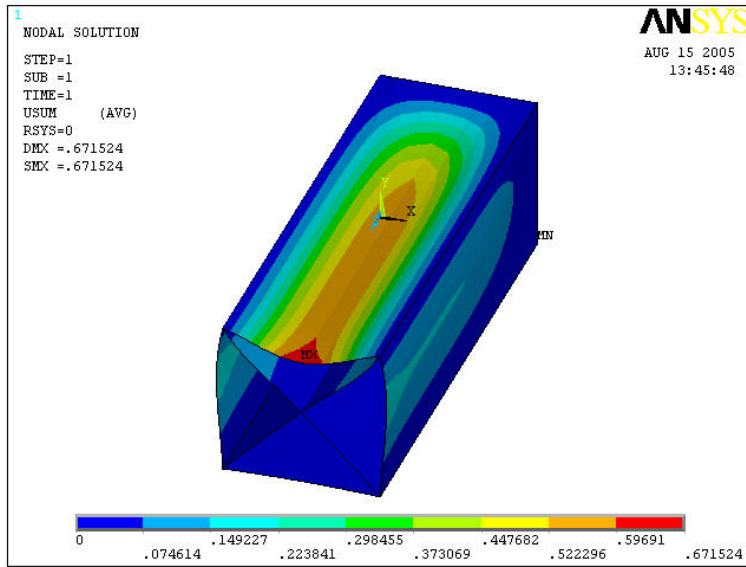


Figure 3.7 X2 Displacement Using ANSYS

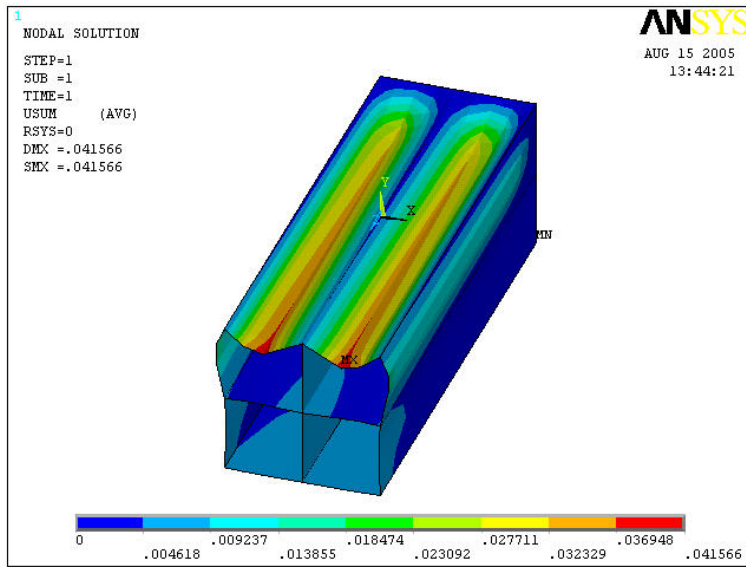


Figure 3.8 Box Displacement Using ANSYS

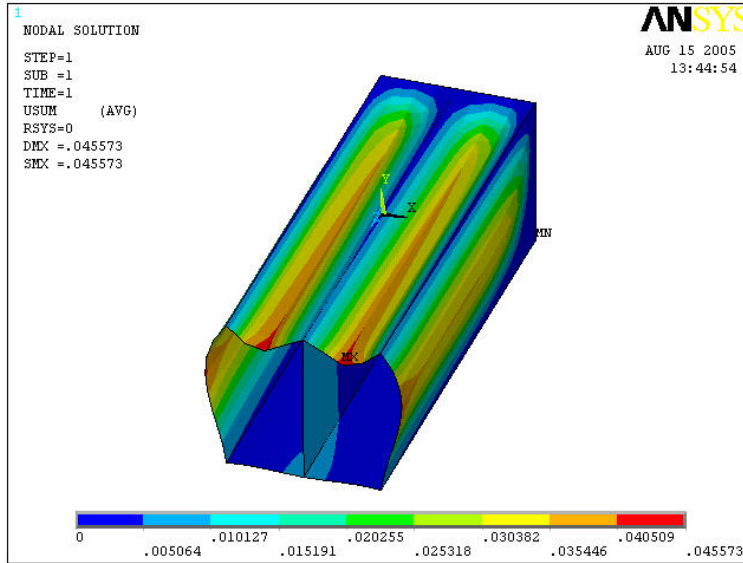


Figure 3.9 Box2 Displacement Using ANSYS

The ADINA generated results are displayed in Figures 3.10 to 3.15. The same loading and boundary conditions were applied to all the cross sections in both ADINA and ANSYS models. The corresponding numerical values of maximum displacements are summarized in Table 3.2.

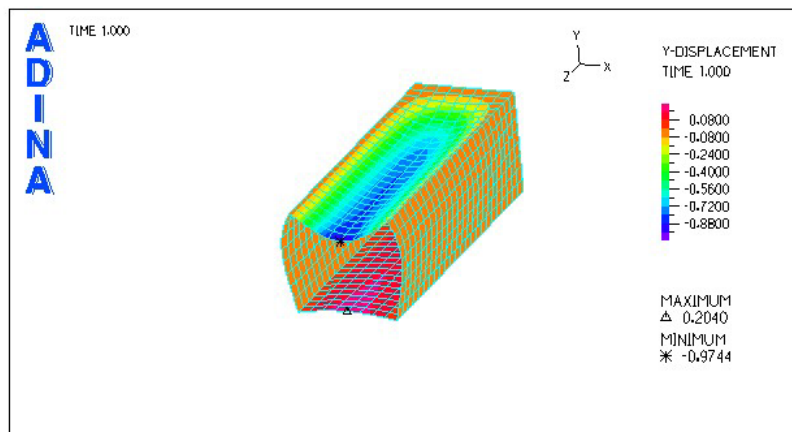


Figure3.10 Tube Displacement Using ADINA

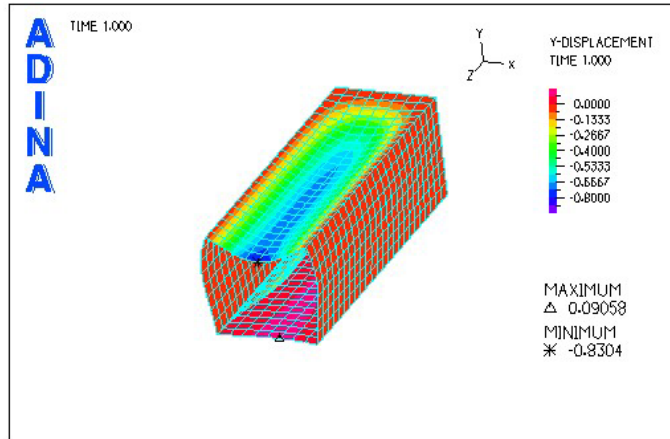


Figure 3.11 Slant Displacement Using ADINA

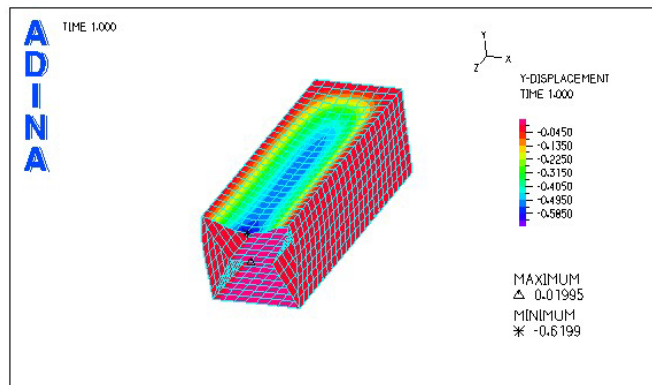


Figure 3.12 X1 Displacement Using ADINA

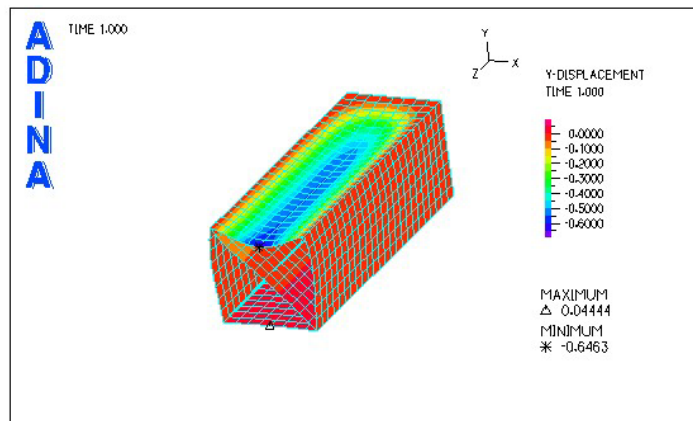


Figure 3.13 X2 Displacement Using ADINA

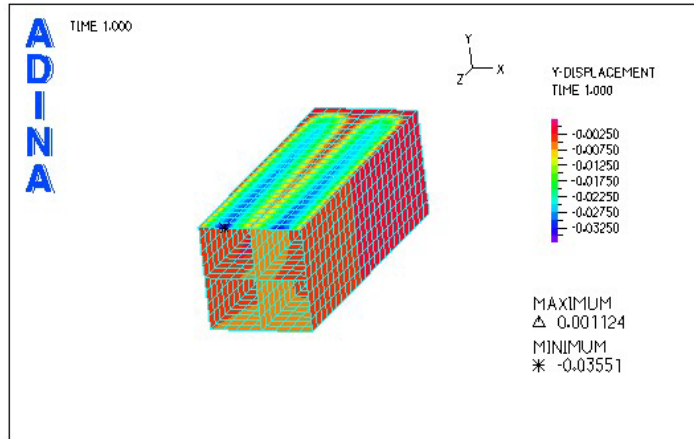


Figure 3.14 Box Displacement Using ADINA

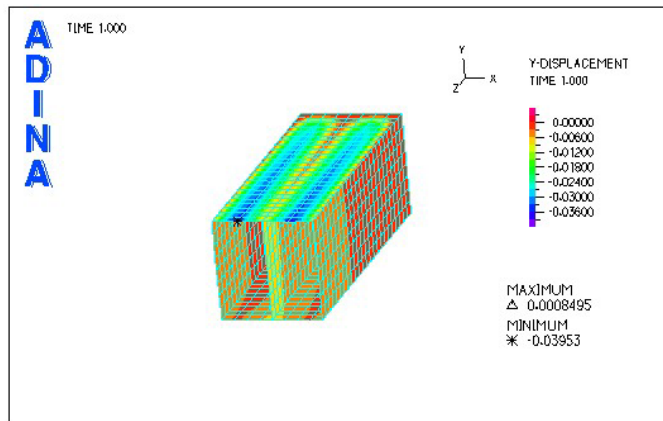


Figure 3.1 Box2 Displacement Using ADINA

Table 3.2 ADINA Bending Results

Cross Section	Maximum Displacement (in.)
Tube	0.9744
Slant	0.9304
X1	0.6199
X2	0.6463
Box	0.0355
Box 2	0.0395



### 3.3.2 Discussion of Finite Element Bending Results

The most effective cross section in regards to bending stiffness is the Box section. This section had a maximum displacement of 0.0355 inches. The least effective cross section for bending resistance is the Tube section. This section experienced a maximum displacement of 0.9744 inches. Comparing the two sections indicates that the Box section is stiffer to bending because of its middle support section, and it reacts with properties comparable to an I-beam. The Box section has a slight advantage over the Box 2 section because of the middle cross segment which restricts a large curvature of the sidewalls in bending. It is important to note that the maximum displacements all occur at the top, center-edge location farthest from the fixed support end.

The Tube section is a commonly extruded section and is easily available in commercial sales. The engineering aspect in question is if using an uncommon section, which requires special production costs, but has higher bending stiffness is worth the cost compared to the tube section's commercial availability and cost benefit? A valid option is to experiment and modify the tube section extrusion by compensating for the higher displacement values with face plates that will create a sandwich panel with bending stiffness capabilities.

### 3.4 Torsion Analysis

A torsional load was applied to the cross sections from Figure 3.1 as depicted in Figure 3.16 and the results were compared by the maximum shear stress reached in each section. Similar to the procedure followed in the bending analysis, all the cross sections were modeled in ANSYS and ADINA with all loading, geometry, and boundary conditions kept constant throughout the analysis. The shell element divisions used in both the bending and torsional analyses were sized at uniform dimensions of 0.5 inches. Uniform element divisions were important in applying a uniform pressure for bending and an equal torsional load distribution from element to element.

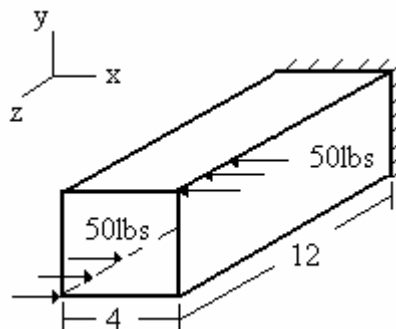


Figure 3.16 Loading Scenario, Dimensions and Boundary Conditions for Torsional Analysis.

Material: Aluminum  
Elastic Modulus:  $26 \times 10^6$  psi  
Poisson's ratio: 0.33  
Loading: 50 lbs on each node  
Elements: Shell  
Element size: 0.5 in.  
Element thickness: 0.02 in.  
Section Dimensions: 4 x 4 x 12 x 0.02 in.

### 3.4.1 Torsion Results

The ANSYS generated results are displayed in Figures 3.17 to 3.22. The results display plots of the maximum stress distributions from an applied load of 50 lbs. The corresponding numerical values of maximum displacements are summarized in Table 3.3.

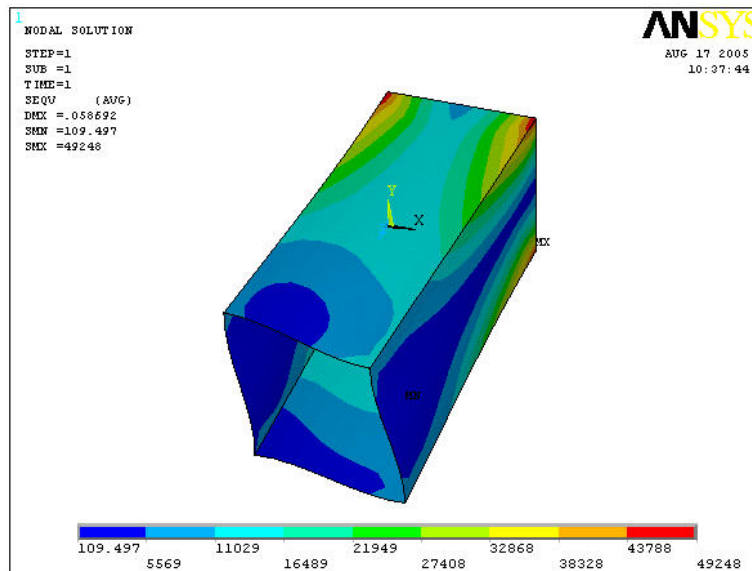


Figure 3.2 Tube Torsion Results Using ANSYS

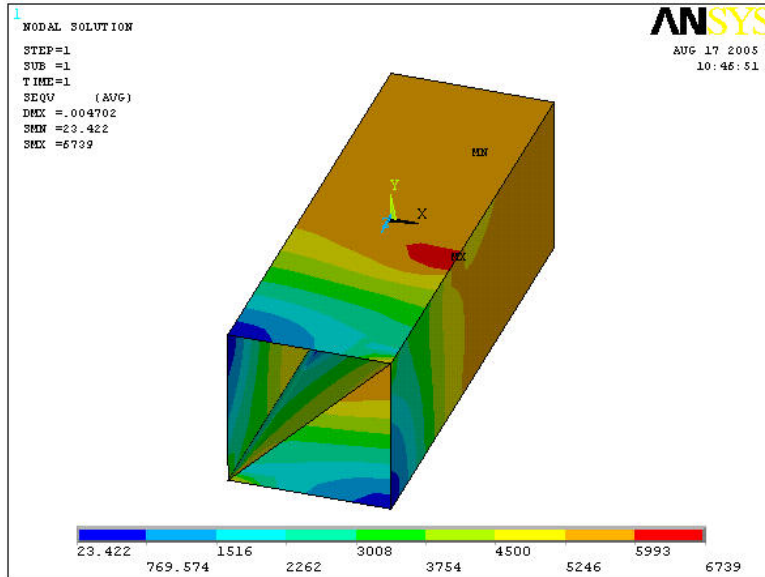


Figure 3.3 Slant Torsion Results Using ANSYS

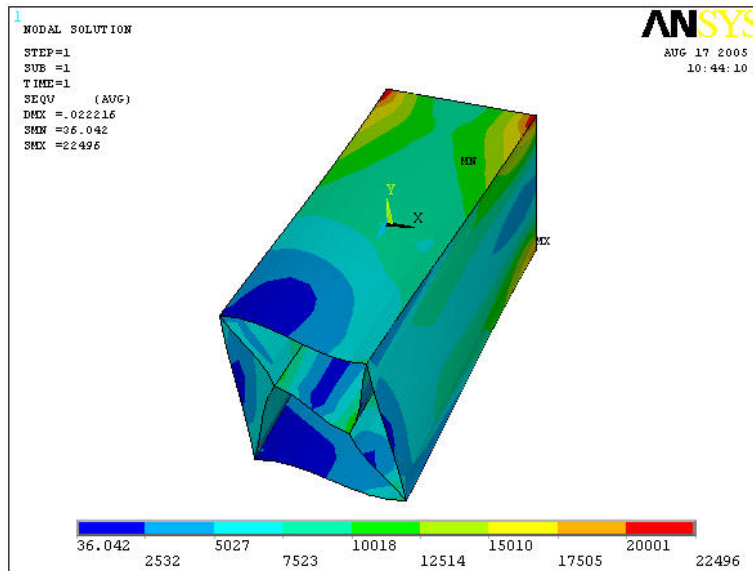


Figure 3.4 X1 Torsion Results Using ANSYS

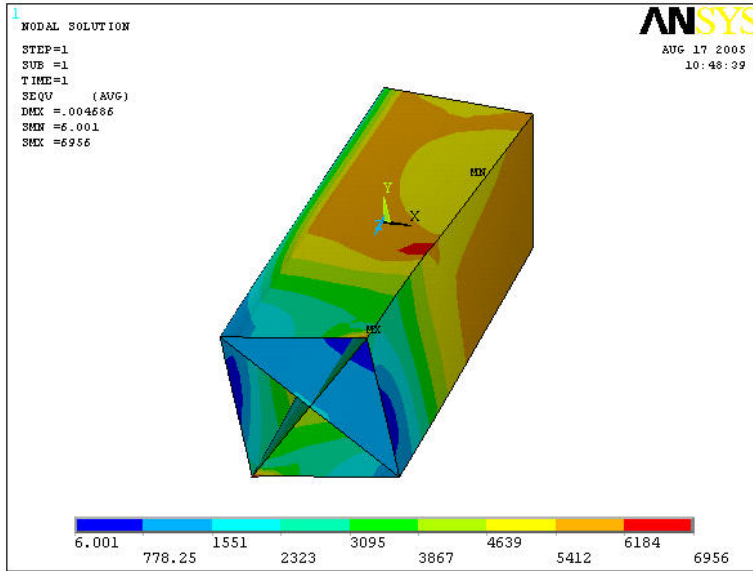


Figure 3.5 X2 Torsion Results Using ANSYS

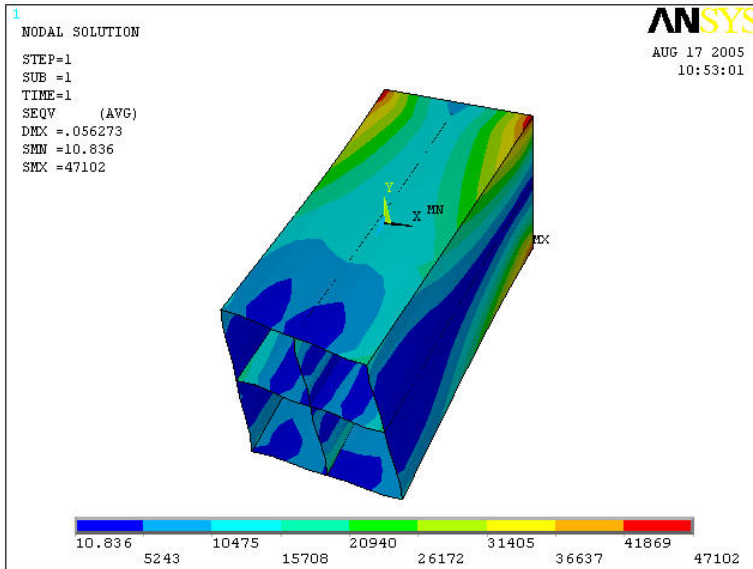


Figure 3.21 Box Torsion Results Using ANSYS

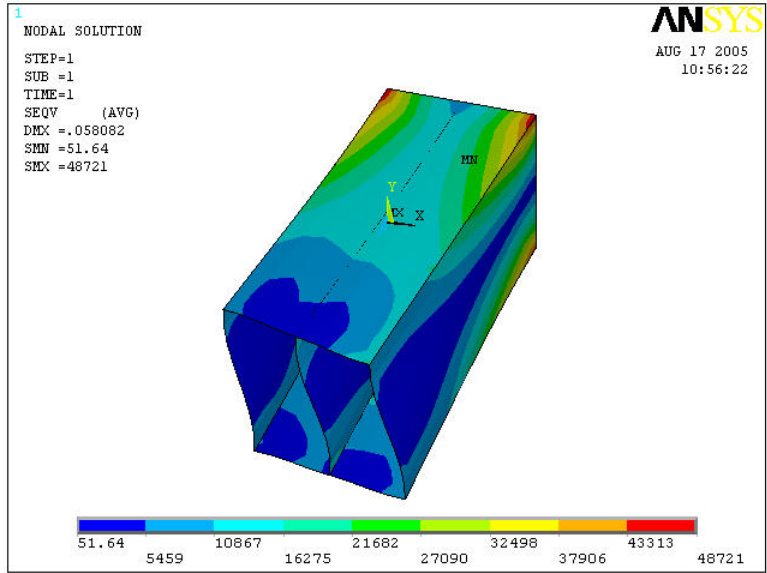


Figure 3.22 Box 2 torsion results using ANSYS

Table 3.3 ANSYS Torsion Results

Cross Section	Maximum Shear Stress (psi)
Tube	49248
Slant	6739
X1	22496
X2	6956
Box	47102
Box 2	48721

The ADINA generated results are displayed in Figures 3.23 to 3.28. The same loading and boundary conditions were applied to the cross sections in both the ADINA and ANSYS models. The corresponding numerical values of maximum displacements are summarized in Table 3.4.

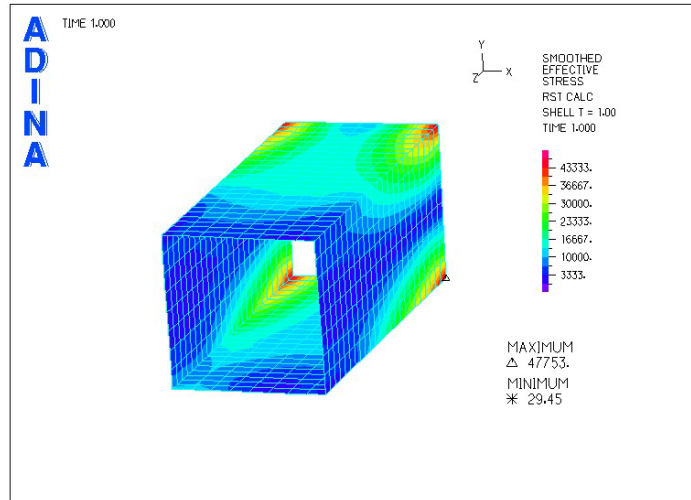


Figure 3.6 Tube Torsion Results Using ADINA

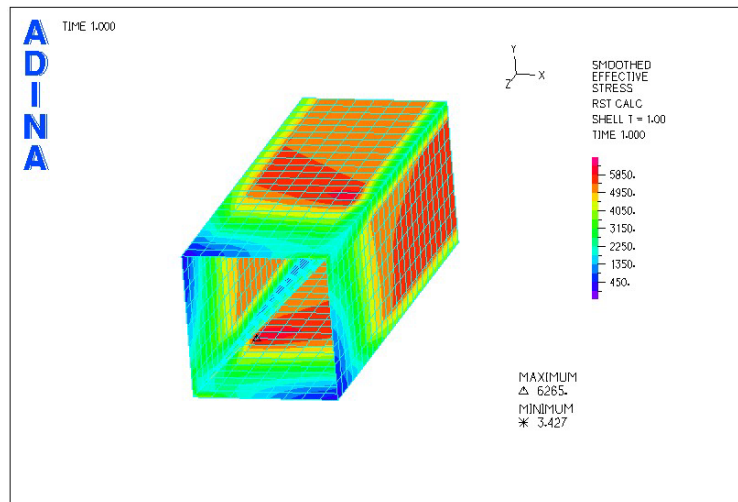


Figure 3.24 Slant Torsion Results Using ADINA

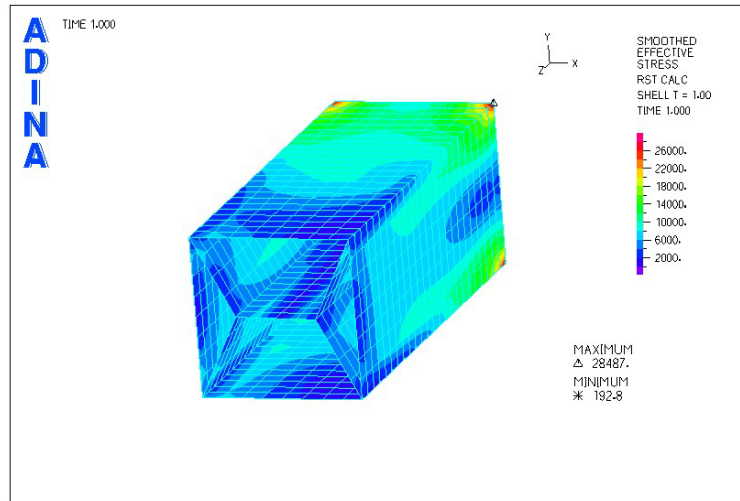


Figure 3.7 X1 Torsion Results Using ADINA

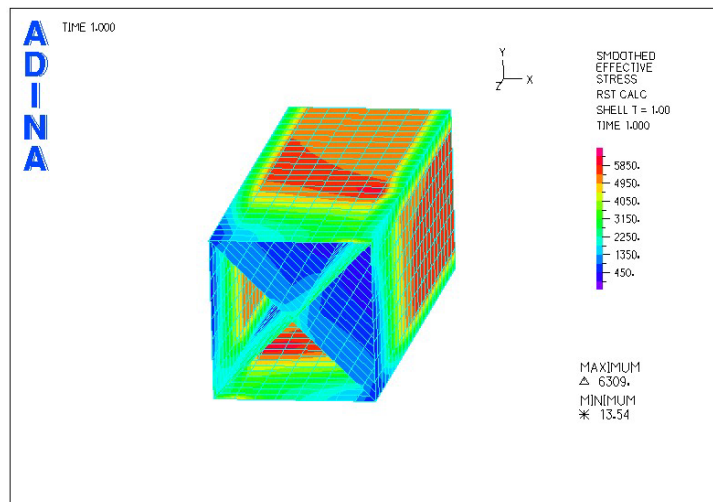


Figure 3.8 X2 Torsion Results Using ADINA

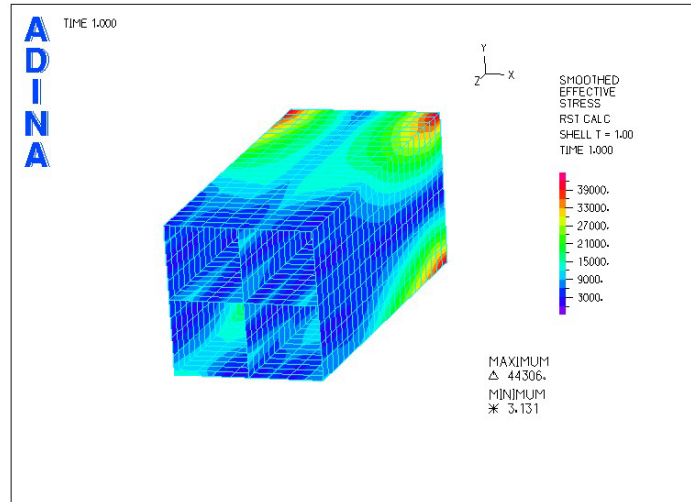


Figure 3.9 Box1 Torsion Results Using ADINA

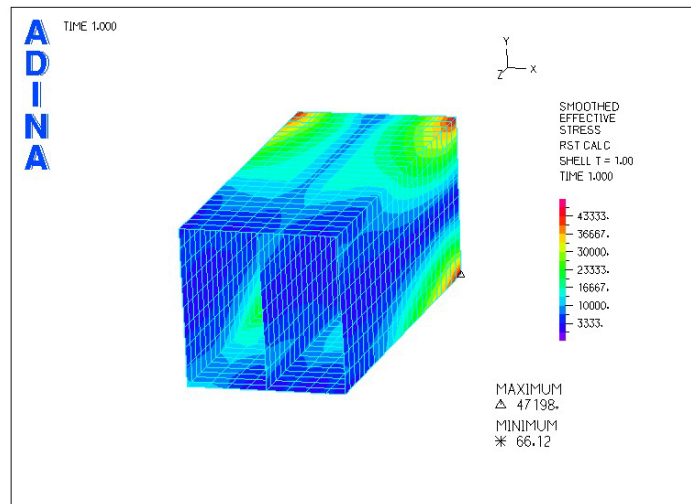


Figure 3.28 Box2 Torsion Results Using ADINA

Table 3.4 ADINA Torsion Results

Cross Section	Maximum Shear Stress (psi)
Tube	47753
Slant	6265
X1	28487
X2	6309
Box	44306
Box 2	47198



### 3.5 Comparison of Bending and Torsion Results

The results of the of the bending and torsional loading in the cross section members are summarized by the bar charts presented in Figures 3.29 and 3.30. The numerical values are also tabulated in Table 3.5. These results indicate that the Slant and the X2 configurations are the most effective designs for minimum stress values, while the Box1, Box2, and Tube sections exhibit the highest stress levels. The diagonal supports that connect to the inside corners of the Slant, X1, and X2 extrusions are effective for resisting the applied torsion.

Table 3.5 Comparison of ANSYS and ADINA Bending and Torsion Results

Cross Section	Bending ADINA	Torsion ADINA	Bending ANSYS	Torsion ANSYS
	Max Deflection	Max Stress	Max Deflection	Max Stress
Tube	0.9744	47753	0.997103	49248
Slant	0.9304	6265	0.854074	6739
X1	0.6199	28487	0.648361	22496
X2	0.6463	6309	0.671524	6956
Box1	0.0355	44306	0.041566	47102
Box2	0.0395	47198	0.045573	48721

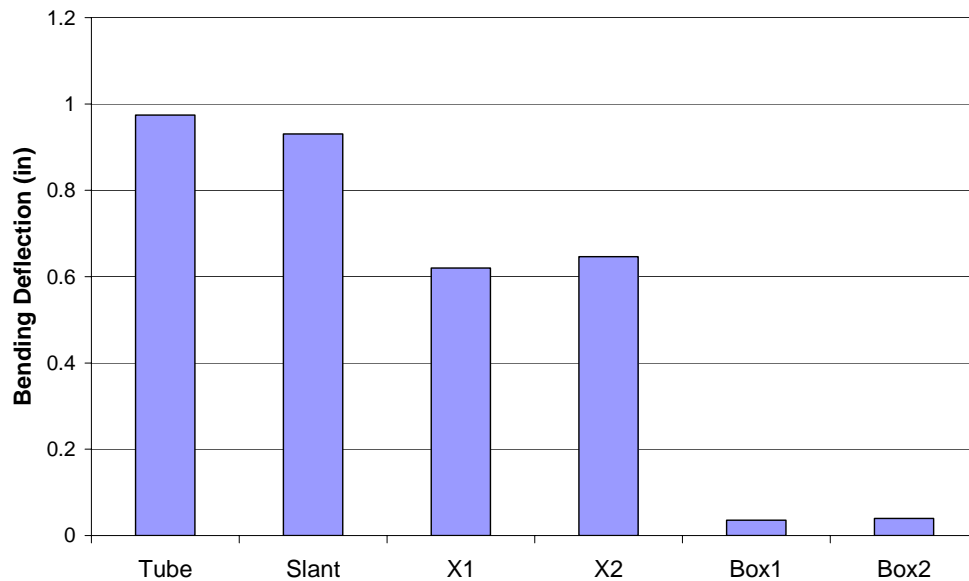


Figure 3.29 Plot of Maximum Bending Deflection for Tube Cross Members

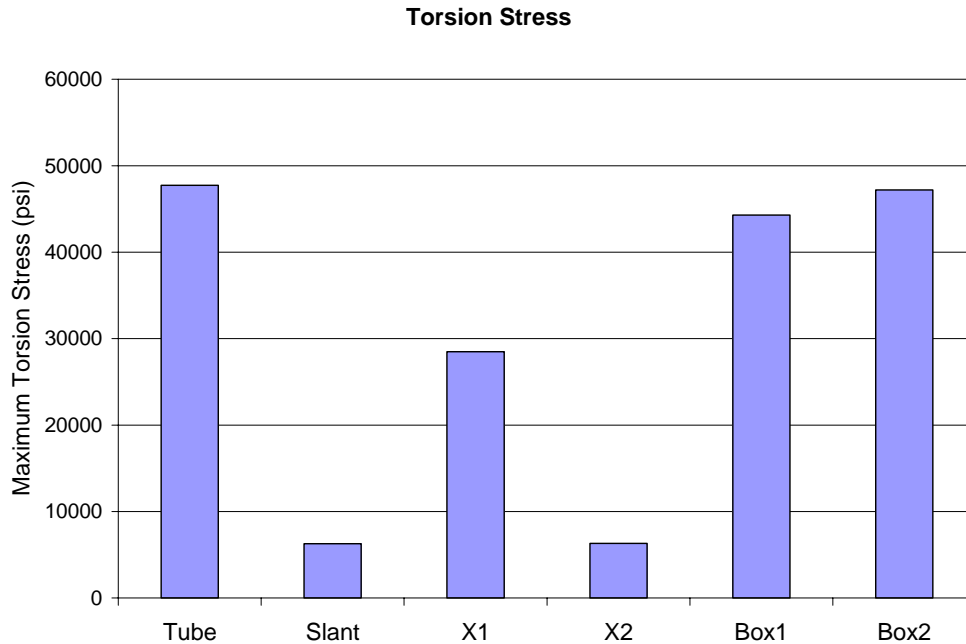


Figure 3.30 Plot of Maximum Torsional Stress within the Tube Cross Members

### 3.6 Weight Comparison

The structural weights of the different cross sections considered in this thesis are compared on the basis of one-square foot section which would be implemented into the trailer flooring. The existing trailer floor weight has also been determined as a baseline for assessing the weight savings achievable by using the sandwich composite design with the various cross sections described above as core materials.

The existing trailer floor is composed of 54 cross member (SI Beams) which are spaced at 1 ft (0.305m), and the length of each is 8ft (2.44m). The cross members contribute a total weight of 4,104 lbs (1861.5 kg). Adding to the cross member weight is the oak floor which contributes 5,227 lbs (2370.9 kg) and covers 432 ft<sup>2</sup>.

#### Cross Beam Weight:

$$54 \text{ cross beams} = 4104 \text{ lbs} \quad \frac{4104 \text{ lbs}}{54 \text{ beams}} = 76 \frac{\text{lbs}}{\text{beam}}$$

$$\frac{76 \frac{\text{lbs}}{\text{beam}}}{8 \frac{\text{ft}}{\text{beam}}} = 9.5 \frac{\text{lb}}{\text{ft}} \quad 9.5 \frac{\text{lb}}{\text{ft}} \times 1 \frac{\text{beam}}{\text{ft}} = 9.5 \frac{\text{lb}}{\text{ft}^2}$$

### Oak Floor Weight:

$$\text{oak floor} = 4645 \text{ lbs} \quad \text{floor area} = 54 \text{ ft} \times 8 \text{ ft} = 432 \text{ ft}^2$$

$$\frac{5227 \text{ lbs}}{432 \text{ ft}^2} = 12.1 \frac{\text{lbs}}{\text{ft}^2}$$

### Trailer Floor Weight per Square Foot:

$$\text{weight of beams} = 9.5 \frac{\text{lbs}}{\text{ft}^2} \quad \text{weight of oak floor} = 12.1 \frac{\text{lbs}}{\text{ft}^2}$$

$$\text{weight per square foot} = 9.5 \frac{\text{lbs}}{\text{ft}^2} + 12.1 \frac{\text{lbs}}{\text{ft}^2} = 21.6 \frac{\text{lbs}}{\text{ft}^2}$$

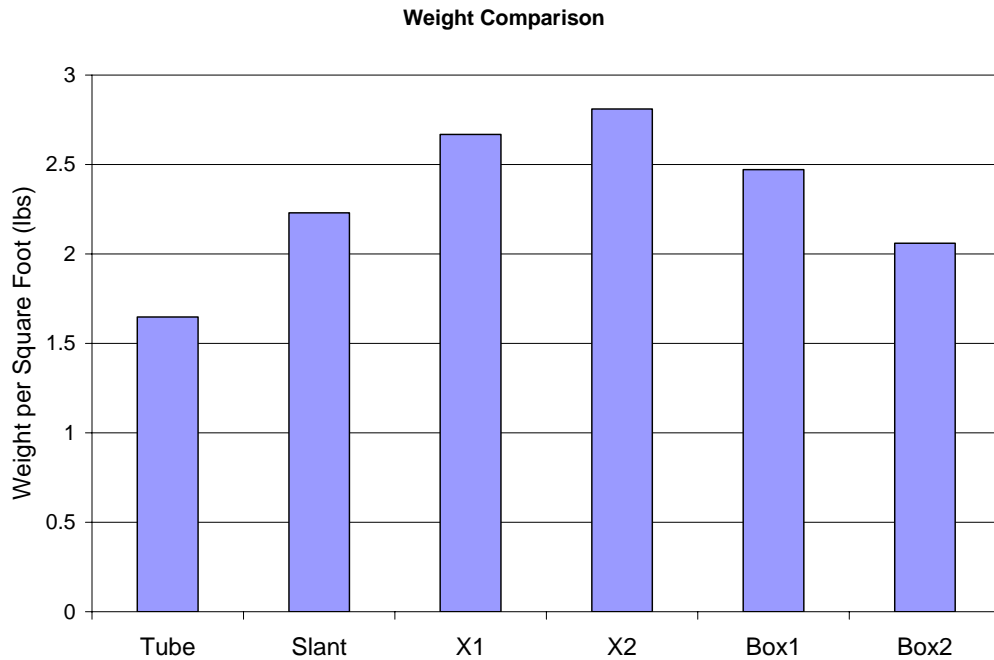


Figure 3.31 Plot of the Weight Comparison between Cross Tube Members

A weight comparison between the alternative cross-section designs are presented in Table 3.6 as well as in the bar chart in Figure 3.31. It can be noticed that adopting any of the new designs to replace just the oak floor ( $12.1 \text{ lb/ft}^2$ ) in the current design results in a significant

weight. The Tube design is the least weight design that satisfies the strength, serviceability, and flexibility requirements.

Table 3.6 Weight Comparisons between Alternative Cross-Sections

<b>Cross Section</b>	<b>Surface Area</b>	<b>Individual Section Weight (lbs)</b>	<b>Square Foot Surface Area</b>	<b>Square foot Weight (lbs)</b>
Tube	192	0.54912	576	1.64736
Slant	259.8	0.743028	779.4	2.229084
X1	311	0.88946	933	2.66838
X2	327.6	0.936936	982.8	2.810808
Box1	288	0.82368	864	2.47104
Box2	240	0.6864	720	2.0592
Trailer Floor	N/A	N/A	N/A	21.6

## CHAPTER FOUR

### PROTOTYPING AND TESTING OF LIGHTWEIGHT STRUCTURAL ASSEMBLIES

#### 4.1 Innovative Structural Joining Configurations

##### 4.1.1 Development of Model Joints and Prototype Designs

The preliminary lightweight design concepts for the flooring design of the trailer are shown in Figures 4.1 to 4.3. Figure 4.1 displays two types of sandwich panel configurations, A and B, for the floor structure of a trailer. Type A consists of a polymer composite top plate with an extruded ribbed composite bottom plate. The combined structure formed by joining these plates provides both a lightweight and stiff floor platform. Type B panel is composed of polymer composite top and bottom plates with aluminum C-channels sandwiched between the plates as the core material. A major advantage of the aluminum C-channel core is that it facilitates the joining of the bogey and the kingpin sections to the floor structure of the trailer. The main disadvantage is the need of bonding between the aluminum beams and the polymer matrix composite panels.

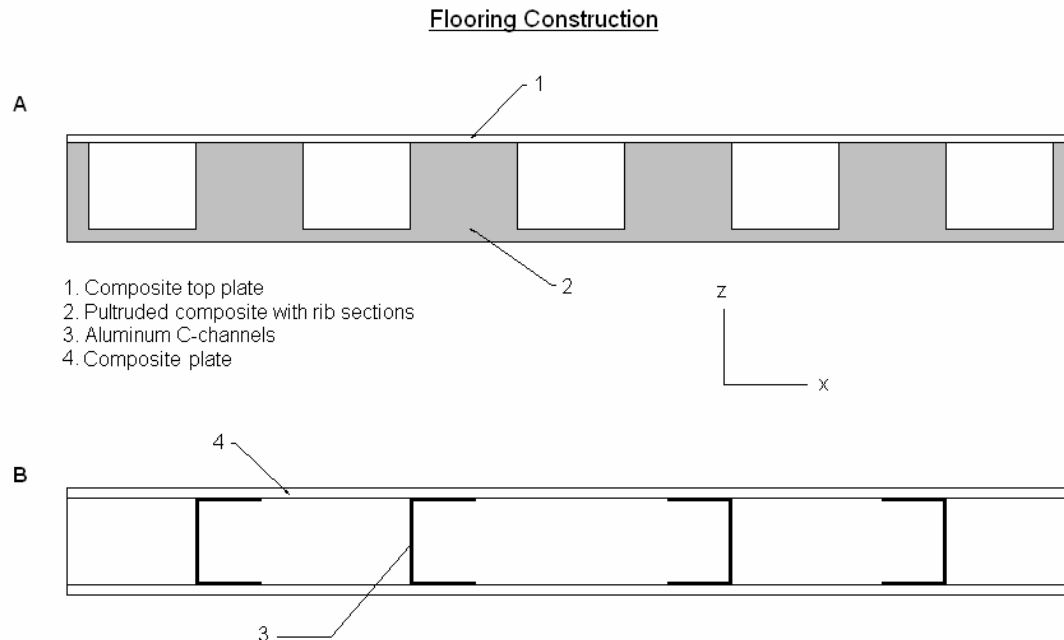


Figure 4.1 Alternative Design Concepts for the Floor Platform of a Modified Van Trailer.

Type C floor construction as shown in Figure 4.2, is comprised of a top and bottom extruded polymer composite plate with small ribbed sections. The small ribbed sections apply a restraint to aluminum or titanium pipes of square cross section. The main advantage of this design consists of the benefit that the top and bottom plate geometry allows for easy joining of metal and polymer composite areas, without complicated and expensive bonding methods. The metal core material provides good accessibility for joining of the bogey and kingpin sections to the flooring structure.

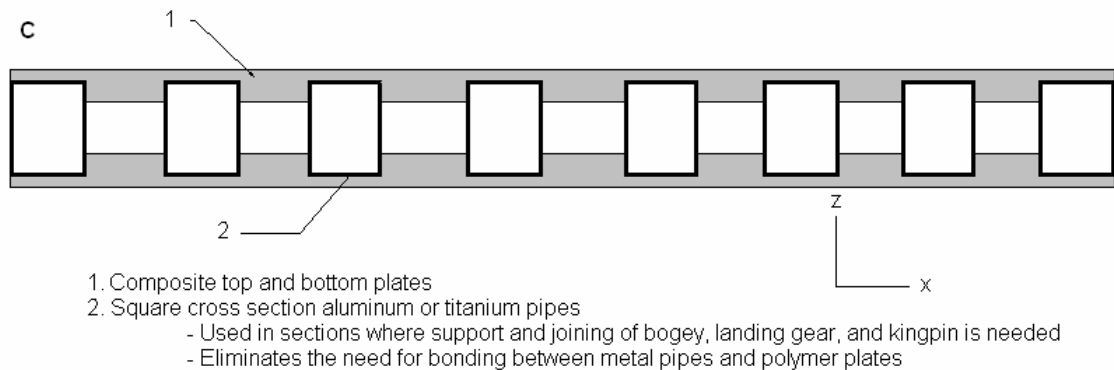


Figure 4.2 Sandwich Composite Structure with Aluminum Tube Core Construction for Flooring Platform Applications. Design concept C.

Type D floor construction, as shown in Figure 4.3, consists of fiberglass I-cross beams connected through fiberglass bearing bars running along the trailer axis through the web centers. The advantages of this type of construction is its good suitability to forming connections at the bearing bar location between the floor panel and the structures above or below the floor. The composite I-beam structure is beneficial as a lightweight design. The addition of top and bottom plate coverings is needed to enclose the I-beam sections which will create a solid flooring platform. The options for the plate coverings will be discussed later in this work through advancements of the I-beam design.

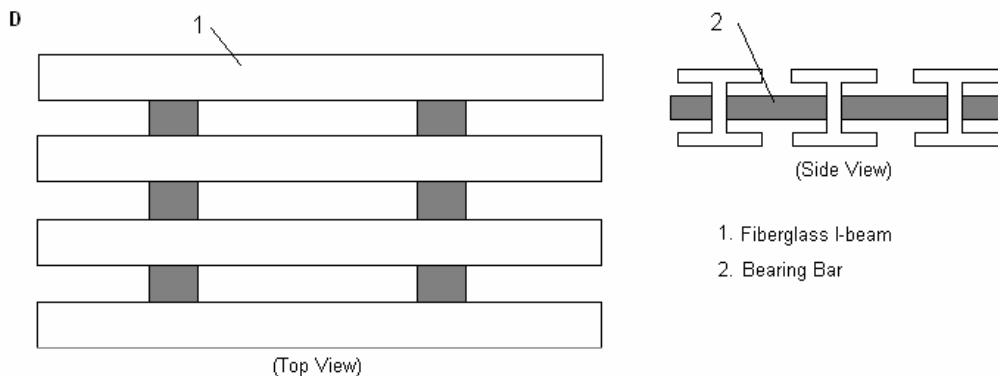


Figure 4.3 Type D Flooring Alternative Using Composite I-Beams as Cross Member Supports and Composite Bearing Bars

The side panels of the scaled prototype trailer are segmented to allow for small sliding and bending deflections throughout the surfaces of the side and top panels. The fiberglass panels forming the sidewall of the trailer are connected by an H-joint that houses two side panels and is reinforced by adhesive bonding in the final design configuration as shown in Figure 4.4.

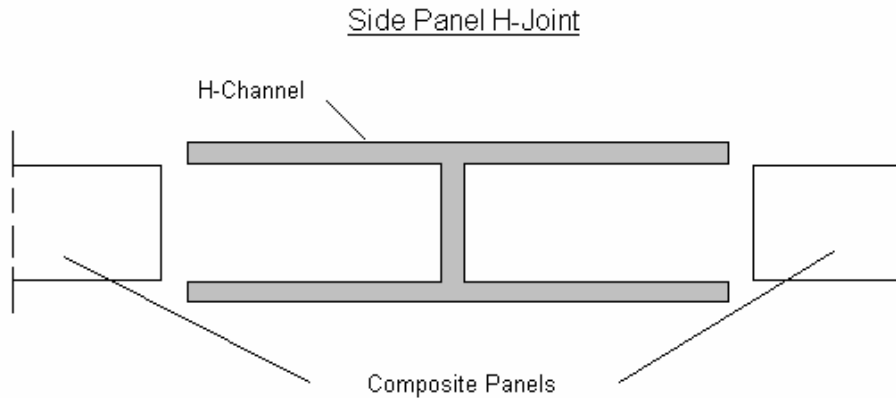


Figure 4.4 Connection Method between Side Panels by an H-Joint Configuration

The double corner joint configuration is utilized to connect the ceiling panel to the side panels as depicted in Figure 4.5. It allows joining by an integrated fit between two sidewall panels and allows for reinforcement by adhesive bonding.

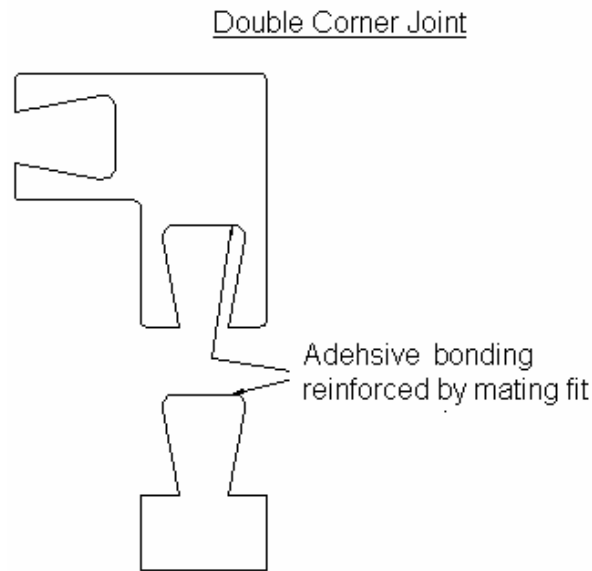


Figure 4.5 Double Corner Joint.

Figure 4.6 shows a configuration for the corner joint connecting the flooring to the side panels. The spacing between the composite top plate and bottom plate of the sandwich flooring platform will house the insert from the joint. In order to allow such a joint configuration, the core material of the sandwich floor panel will not run the full width of the floor, so that sufficient

room is available for the insert. Adhesive bonding will aid the structure in this case and secure the integrity of the joint between the side and bottom plates.

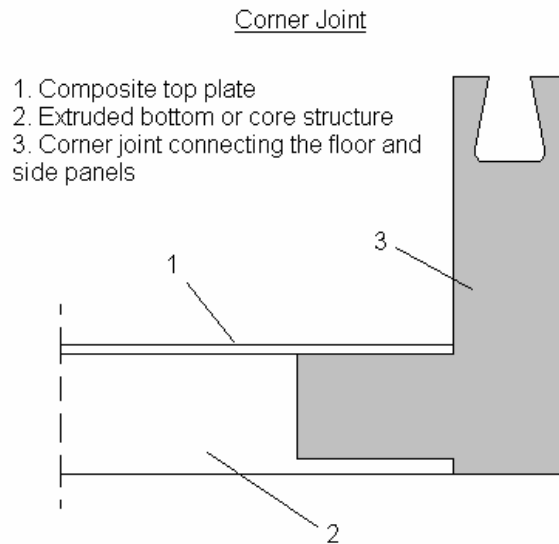


Figure 4.6 Corner Joint for Connecting the Floor Platform to the Sidewall or Side Panels of a Van Trailer

An alternative option for the corner joint involves two fiberglass angles that are adhesively bonded to the I-cross beams of the floor and side panels as shown in Figure 4.7. The legs of both the interior and exterior angles are bonded to the floor and the vertical sections of the angles are bonded to the side panels of the trailer.

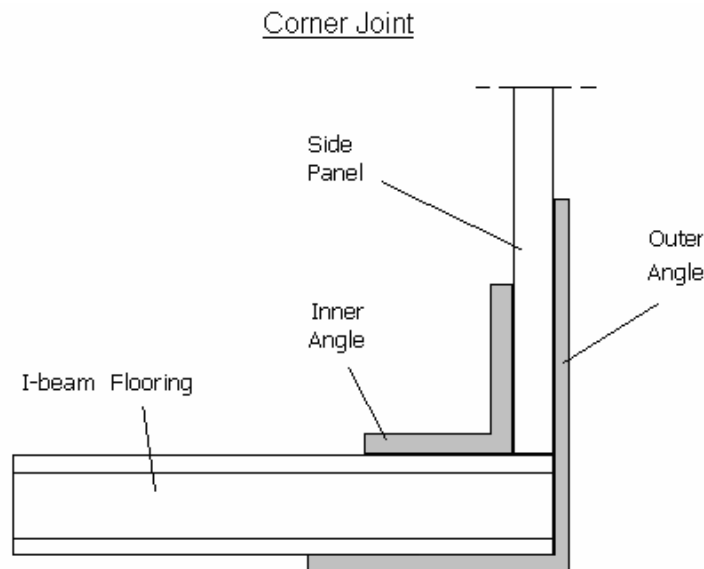


Figure 4.7 Alternative Option for the Corner Joint Connecting the Side Panels to the Flooring Platform



The trailer has been designed to be modular, which allows sections to be removed and replaced. This design concept ultimately reduces the transportation weight of the trailer. Three segments in the trailer are removable. In the model, the sections are each 1 foot sections. For a standard 48 ft. trailer, the three removable sections will be 4 ft in length and allow for a resulting trailer ranging in length from 36 ft to 48 ft in increments of 4 ft. More on the modular design will be discussed later.

The method of connecting the segments in the trailer will vary with the different concepts for the flooring structure. The segment connection studied in this report and used in the model is for the I-cross beams and bearing bars floor design (type D).

## **4.2 Prototyping of Innovative Structural and Joining Concepts**

A prototype of a van trailer was constructed at a 1 to 4 scale. The main purpose of building a solid model is to investigate experimentally in simulated conditions the potential benefits and drawbacks of various joining configurations and sandwich composite implementation. The constructing and structural testing of such a model provides reliable, extensive data for comparative assessments of alternative joining methods and material selection, mostly through finite element modeling and analysis.

The primary design criteria guiding the fabrication of a scaled trailer prototype are the achieving of optimal tradeoffs between structural weight and performance, based on extensive use of lightweight, strong and durable components, connected by fastener-free joints that allow easy assembly and maintenance. The construction of the prototype model involves optimum tailoring of fiberglass composite panels, I-beams, and angles to meet typical design specifications. A hybrid combination of aluminum and fiberglass components has been used as a preliminary step towards designing and prototyping an advanced trailer structure. This approach is cost effective and will provide the means to implement high performance advanced sandwich structures into the model design after the initial fabrication process has been completed and studied.

### **4.2.1 Manufacturing Process**

The building of the prototype model was performed in distinctive phases in order to allow continual assessment of the feasibility, potential advantages and disadvantages of different design configurations. Phasing of the fabrication process allowed incremental improvements in the design and fabrication concepts. The first phase was the construction of the rear section of the trailer model. The process of fabricating this section progressed into the following trailer sections and provided an effective method to culminate the full trailer model design

The following commercial parts and materials have been used thus far in the construction of the trailer prototype:

- ¼” thick fiberglass panels
- 1” Standard fiberglass I-beams
- Fiberglass bearing bars
- Fiberglass angles
- Anodized aluminum H-channels
- Anodized aluminum J-channels
- Anodized aluminum U-channels
- Anodized aluminum cornering channels

Custom carbide tipped tools were used to cut the fiberglass panels and the I-beams in order to tailor each to the design specifications of the trailer. The fiberglass panels are used to build the top and side walls of the trailer. Cross I-beams are the main structural elements of the floor and are designed to carry the static and dynamic loads applied on the trailer bed during its commercial operation. The assortment of fiberglass I-beams is reinforced by fiberglass “bearing bars” which run the length of the trailer and connect the I-beams through the web of each. Besides providing structural reinforcement, the fiberglass bearing bars will provide connection points for the bogey, landing gear and kingpin of a trailer. Aluminum H-channels and edge corners were manufactured and tailored to provide strong connections between adjacent side panels, as well as between the side and top panels. The H-channels are anodized aluminum with ¼” openings to fit the thickness of the side panels. The H-channels had to be cut to the proper height and trimmed properly to allow proper spacing and matching with the corner edge trim. The U-channels and the J-channels are used as trim sections for the rear door of the trailer.

The side panels have been bonded in order to secure the integrity of the H-channel joints. Furthermore, the side panels of the trailer have been segmented to allow structural flexibility and effectively absorb typical static, thermal, and dynamic forces associated with typical loading scenarios. All the structural joints in the trailer will be secured by adhesive bonding methods. The bonding process requires sanding or roughing of areas in contact, following by thorough cleaning of the bonded areas. *Araldite 2021* toughened methacrylate adhesive was used to bond the fiberglass to metal components. The main advantage in choosing *Araldite 2021* is that it provides a bond that fills voids and gaps between the mating parts and it also exhibits elastic characteristics in its cured state. The bonding between fiberglass angles and fiberglass panels was done with epoxy for secure adhesion.

#### **4.2.2 Model Trailer**

Figure 4.8 shows a section the trailer model and the different types of joints, channels, and angles that comprise the trailer model as described previously. Figure 4.8 shows the model in early stages of development and only displays the front section of the trailer. Bonding and joining of the structure was the final phase in the manufacturing process. Once completed, the three sections of the trailer were complete and shown figure 4.9.

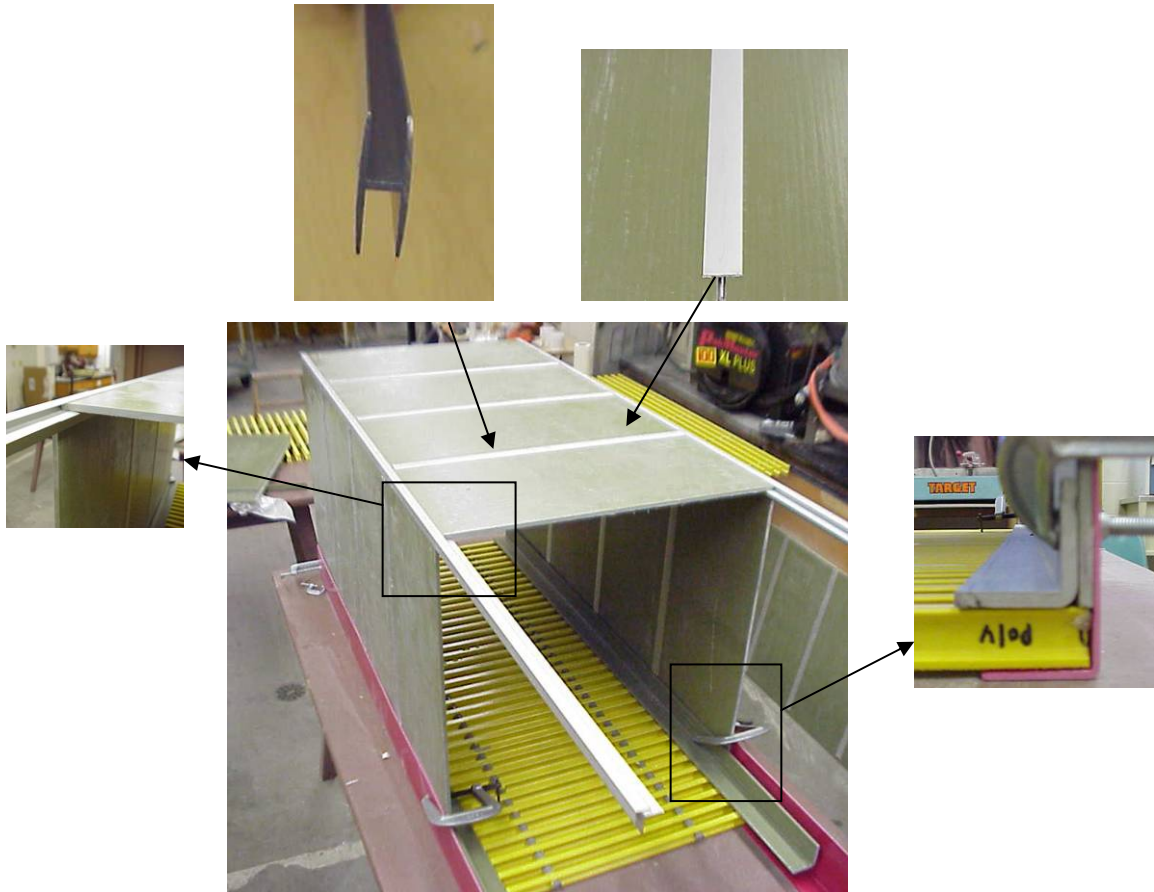


Figure 4.8 Scaled Prototype of the Replica 1:4 Trailer Model Emphasizing the Locations and Types of Joints



Figure 4.9 Unassembled Sections of the Model Trailer

### 4.2.3 Modular Design

The concept of creating a modular trailer design, in which sections of the trailer could be removed if unused, must be facilitated with adequate mechanical joining structures. The main area for connecting the middle segments and the front and rear sections of the trailer are the flooring cross beams. The cross beams in each segment are joined by “beam connectors” which are shown in figure 4.10. The connectors join the segments by securing the flanges of three consecutive I-beams to a reverse U-channel.

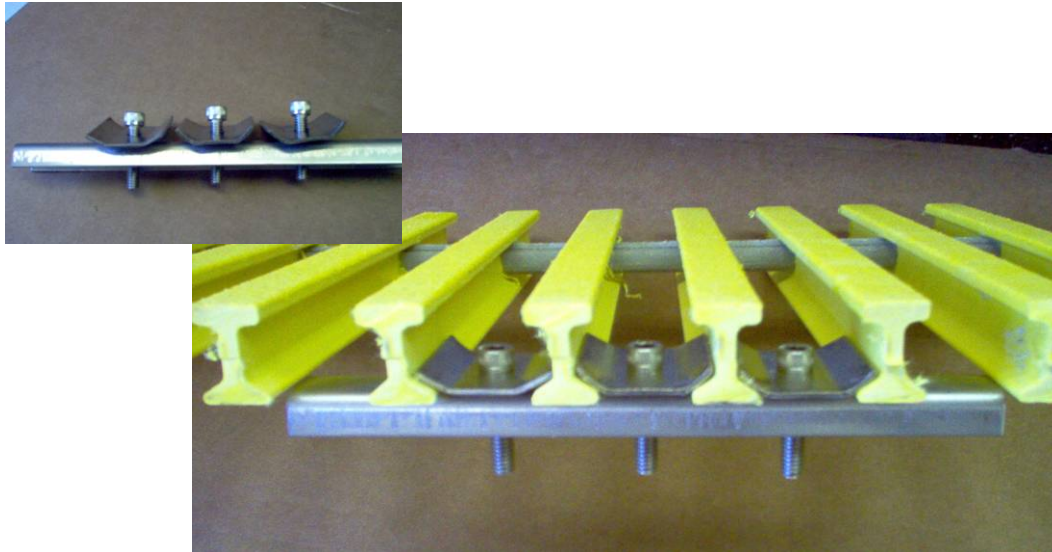


Figure 4.10 Method of Joining the Segments of the Van Trailer by Connecting the I-Beam Cross Members



Figure 4.11 A Method to Assist the Joining of Segments for the Modular Application of the Van Trailer Design

A method to assist the beam connectors in joining the trailer segments is shown in Figure 4.11. This concept involves an extension of the interior angles and the top edge rails of the double corner joint. The angles and edge rails of one segment will extend onto the flooring and side panels of the adjacent segment providing added stability and rigidity to the modular design.

### **4.3 Panels with Tube Section Cross Members**

The prior analysis of various cross section aluminum extrusions as a load bearing component for heavy vehicle flooring, presented in Chapter 3, indicated that the concept of using this structural design is promising, which initiated further study. To pursue such investigation, different panel configurations were manufactured for use in experimental testing and finite element modeling.

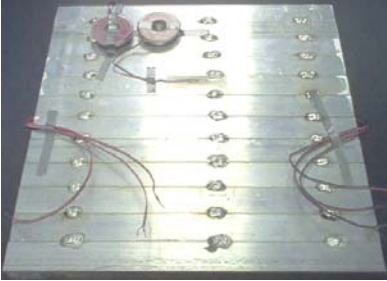

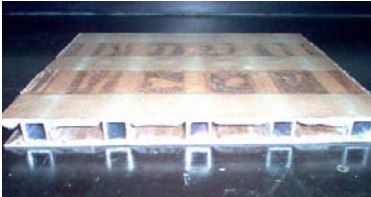
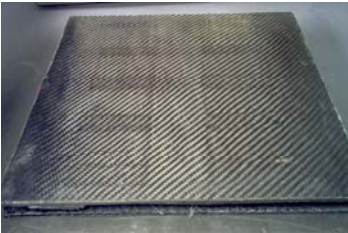
The objective of this phase of research is to find a design that incorporates the bending resistance and weight saving capabilities of the extruded sections and also produces a lightweight structural platform. The initial panel design consisted of a repeated pattern of the different cross sections. However, to maximize weight savings and still maintain loading resistance, different configurations of the cross members were studied.

For this purpose, scaled models of structural design concepts for floor assemblies have been developed and prototyped, instrumented, and tested in the laboratory environment, in order to validate the predictions of the theoretical models. These models were developed as a means to predict and understand the actual performance of the various floor design configurations, either in the form of cross member panels or sandwich composite panels. Each design panel configuration consists of face plates, either aluminum or composites, and a core of extruded aluminum tubes. The main features of the developed panels are summarized in Table 4.1.

Static loading was performed on the four test panels to determine the strains occurring at critical locations and the overall displacement that each panel will yield under the testing procedure. Each panel was simply supported along its respective side edges and loaded in the center of the panel under a 2" by 3" pressure area load. The maximum load reached was 600 pounds.

The experimental results are used to validate the theoretical finite element models, as well as to explore the feasibility and the manufacturing aspects of new, lightweight floor designs. Thus, all the panels were instrumented to measure that their structural response and at the critical location, to generate reliable data for correlations with the theoretical predictions.

Table 4.1 Configurations of Sandwich Panel Prototypes

Structure	Features
<p data-bbox="365 273 552 336"><b>TUBEPLATE</b></p> 	<p data-bbox="706 367 1339 462">12in x 12in x 1in thick plate; 12 Aluminum tube cross members are aligned together along their sides and welded</p> <p data-bbox="706 493 1380 630">The Tubplate design is intended to be an inexpensive and easily manufactured alternate flooring design. The design is tested as a core structure for a sandwich composite design.</p>
<p data-bbox="365 724 552 756"><b>TUBEGRATE</b></p> 	<p data-bbox="706 724 1364 892">12in x 12in x 1in thick plate; 6 Aluminum tube cross members are spaced 1in. apart and contained by U-channel edge rails on each side. Welds are placed on the top and bottom locations where the cross members meet the U-channel edge rails.</p> <p data-bbox="706 934 1380 1029">An inexpensive design which can be easily manufactured. The Tubegrate concept is used as the core structure in the composite sandwich designs that follow.</p>
<p data-bbox="365 1102 552 1134"><b>FIBERPLATE</b></p> 	<p data-bbox="706 1092 1380 1260">12in x 12in x 1in thick plate; 5 Aluminum cross members are used as the core structure which is enclosed by fiberglass face plates. The faceplates have paper honeycomb, ribbed sections between the core members.</p> <p data-bbox="706 1291 1380 1428">A sandwich composite which implements a core structure that increases bending stiffness. The geometry of the face plate creates a joining solution between the metal core and composite face plates.</p>
<p data-bbox="341 1491 576 1522"><b>CARBONPLATE</b></p> 	<p data-bbox="706 1501 1380 1669">12in x 12in x 1in thick plate; 5 Aluminum cross members are used as the core structure which is enclosed by carbon fiber face plates. The faceplates have paper honeycomb, ribbed sections between the core members.</p> <p data-bbox="706 1701 1380 1774">The Carbonplate is the same design as the Fiberplate with carbon fiber being used instead of fiberglass.</p>



## 4.4 Testing of Sandwich Panel Prototypes

### Tubeplate

The *tubeplate* was designed specifically to provide a low-cost, lightweight, and manufacturing efficient alternative to the existing flooring structure. The aluminum tubes are connected by a row of small welds that butt the sides of the square cross section tubes together. The main concern before experimentally testing the *tubeplate* were if the welds would effectively sustain the applied load and if the overall panel would sustain a concentrated load as used in the testing procedure.

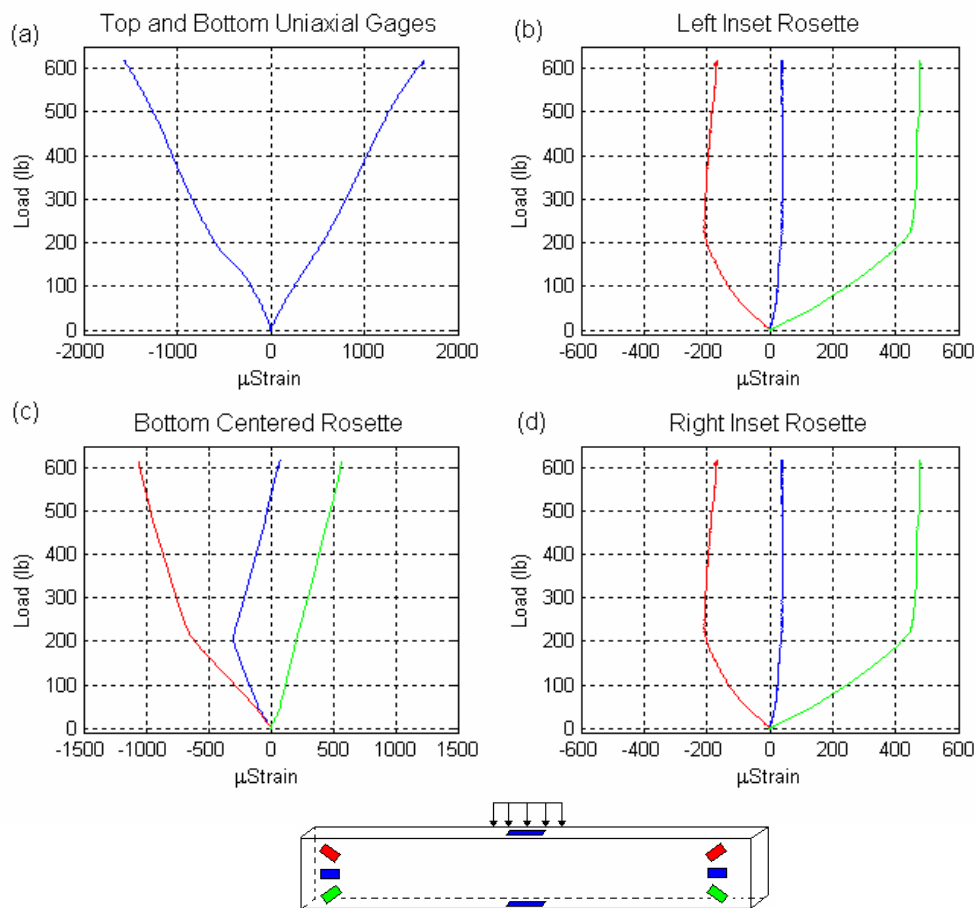


Figure 4.12 Load vs. Strain Plots of the *Tubeplate* Experimental Test

The strain values shown in Figure 4.12 depict the load bearing reaction of the *tubeplate* design. The uniaxial gages in Figure 4.12 (a) show maximum bottom and top strain values of approximately 1600 and -1600  $\mu$ Strain. Figure 4.12 (b) and (d) display the rosette strain values on both the left and right side of the load. The color of the plotted data lines corresponds to the

illustration in Figure 4.12 of the strain gage placements on the cross member closest to the center of the load. Examining Figure 4.12 (b) and (d) reveals that the bottom rosette gage (green) experiences tension throughout the loading process and reaches a maximum strain value of 477  $\mu$ Strain while the top rosette strain gage (red) is in compression and attains a maximum strain value of -208  $\mu$ Strain.

The strain values acquired from the strain gage rosette configurations were used to calculate the shearing strain at this location. The right and left strain gage rosettes were placed on the inset of the simply supported edges which is the location where maximum shear will occur during loading. The  $\gamma_{xy}$  shear strain values throughout the loading process are shown in Figure 4.13. The plot in Figure 4.13 verifies that the shearing strain values increase steadily as the load varies between 0 and 600 (lbs). The maximum strain value at this location is 271  $\mu$ Strain.

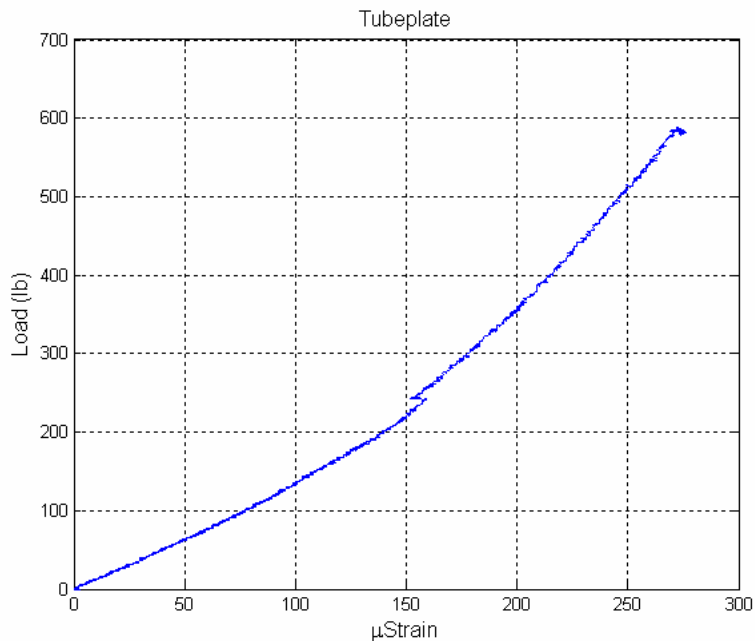


Figure 4.13 Shearing Strain Values for the *Tubeplate* Configuration at the Inset of the Simply Supported Edges

## Tubegrade

The *tubegrade* panel was specifically designed to be a cost and weight effective variation of the *tubeplate* panel. The concept for cost and weight reduction is to reduce the amount of cross members used in the design and add two U-channel edge rails to secure the cross members by welds at their joints. This reduces the amount of material used which in turn reduces the cost. Also, the configuration of the *tubegrade* setup reduces the number of welds needed from 66 for



the *tubeplate* to 24 for that of the *tubegrade*. The structure of spaced aluminum tube cross members are the core structure of the FRP sandwich panels and are tested without top and bottom faceplates to understand their effectiveness as a core material.

A concern before testing was if the small welds will effectively sustain the stresses and strains occurring during loading and how reducing the amount of cross members and adding the edge channel connection will compare to the *tubeplate* design.

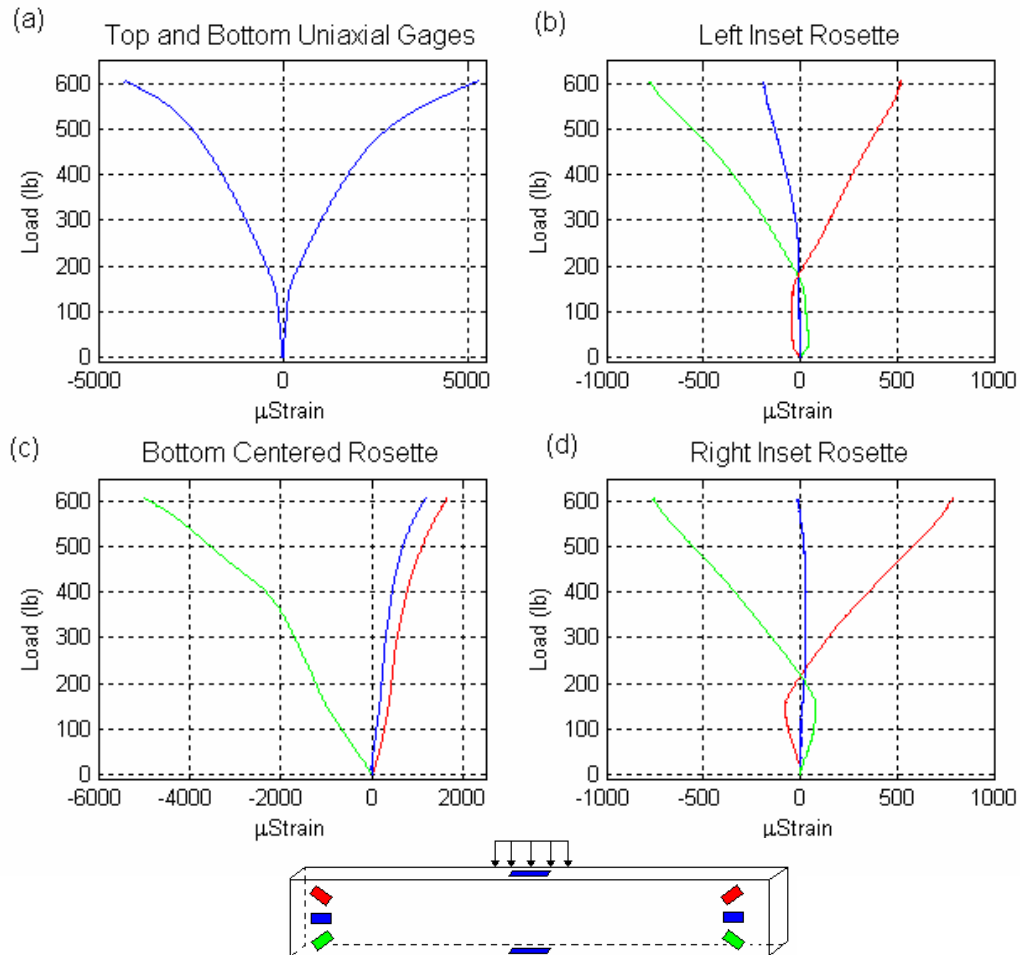


Figure 4.14 Load vs. Strain Plots of the *Tubegrade* Experimental Test

The uniaxial strain gage results shown in Figure 4.14 (a) have a maximum compression value (top gage) of  $-4268 \mu$ Strain and tension value (bottom gage) of  $5239 \mu$ Strain. These values are more than two times the magnitude of the previous uniaxial results from the *tubeplate*,

see Figure 4.14 (a). The higher strain values are a result of the load being distributed over fewer cross members which increases the displacement at these strain gage locations.

An interesting characteristic of the strain gage rosette data in Figure 4.14 (b) and (d) is variation from tension to compression by the top (red) and bottom (green) rosette gages. The change in strain direction is due to the U-channel edge supports of the *tubegrate*. The panel first deforms against the simply supported edges of the test fixture and once the load reaches a critical point, in this case 221 (lbs) the panel begins to deform against the edge of the U-channel supports which changes the direction of the strain. The maximum strain values for the top (red) and bottom (green) gages are 779 and -747  $\mu$ Strain, respectively.

The shear strain on the inset of the simply supported cross member in the *tubegrate* was determined. The Load vs.  $\mu$ Strain plot occurring at the most critical location is shown in Figure 4.15.

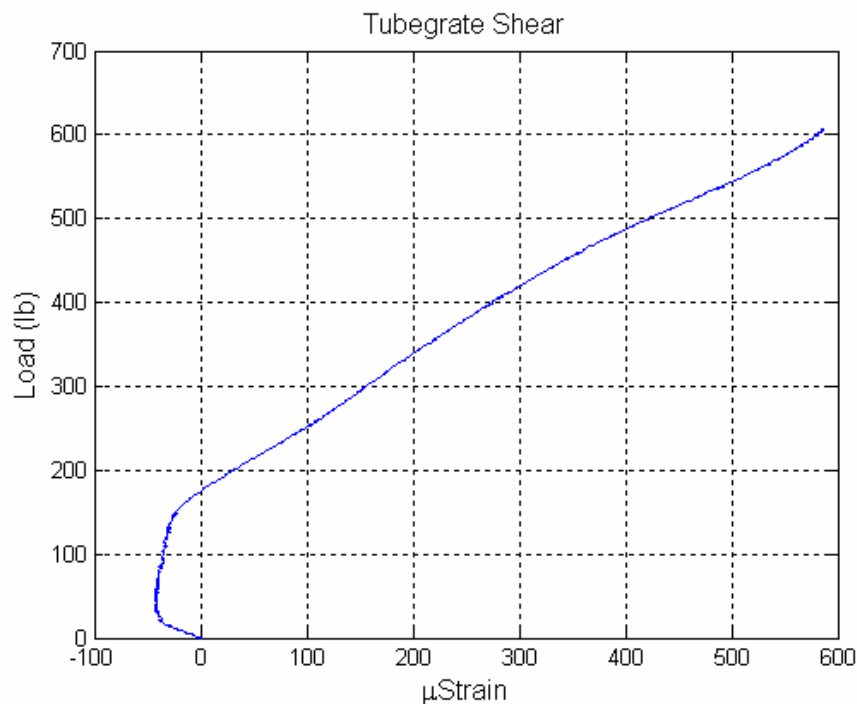


Figure 4.15 Shearing Strain Values for the *Tubegrate* Configuration at the Inset of the Simply Supported U-Channel Edges

The shear stain values in Figure 4.15 differ significantly from those of the *tubeplate* in Figure 4.13. Figure 4.15 shows the change in direction corresponding to the plots in Figure 4.14 (b) and (d), previously discussed and a fairly linear relation between load and strain between load values of 150 (lbs) to 600 (lbs). The maximum shearing strain reached is 587  $\mu$ Strain. In comparison to the *tubeplate*, it can be postulated that the *tubegrate* configuration attains higher strain values at the location of the strain gages. The *tubegrate* design with the edge channel incorporated focuses the shearing strain directly on the inset of this edge. Concluding that the

amount of supporting cross members is half that of the *tubeplate* reveals that the strain values twice as high in magnitude in comparison.

## Fiberplate

The fiberplate panel incorporates the *tubeplate* design as the core structure with the addition of fiberglass top and bottom composite plates. The top and bottom plates also contain ribbed sections (See Table 1). It is important to note that the size of the square tube cross sections in the fiberplate is  $\frac{3}{4}$  inches compared to a 1 inch section in the *tubeplate* and *tubeplate* designs. The difference in sizes allowed for a total 1 inch thickness between all panels, therefore, the overall panel thickness was held constant throughout the test procedures.

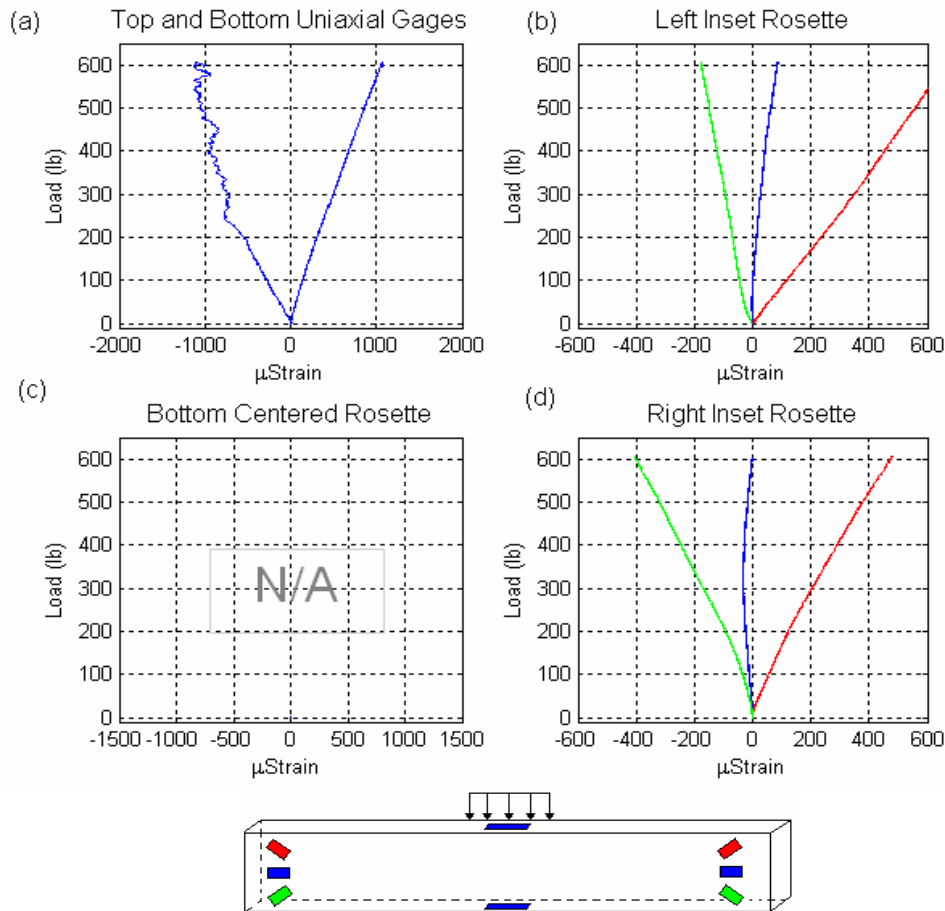


Figure 4.16 Load vs. Strain Plots of the *Fiberplate* Experimental Test

The uniaxial strain gages shown in Figure 4.16 (a) have a maximum compression value (top gage) of  $-1003 \mu\text{Strain}$  and tension value (bottom gage) of  $1069 \mu\text{Strain}$ . These values are approximately five times lower than the strains at this location in the *tubeplate* panel. This

means that the addition of the top and bottom fiberglass composite plates were effective for increasing the panel stiffness and reducing the strains induced by mid-plate bending.

The plots for the bottom rosette, Figure 4.16 (c) are not available because the panel was tested on the opposing side due to fiber damage. The rosette on the opposite had to be removed to apply the load to the center of the plate. This did not hinder the analysis or test procedure.

The shear strain plot was determined in the same manner as the previous tests. The results of the shear strain attained at the inset of the simply supported area can be seen in the Figure 4.17.

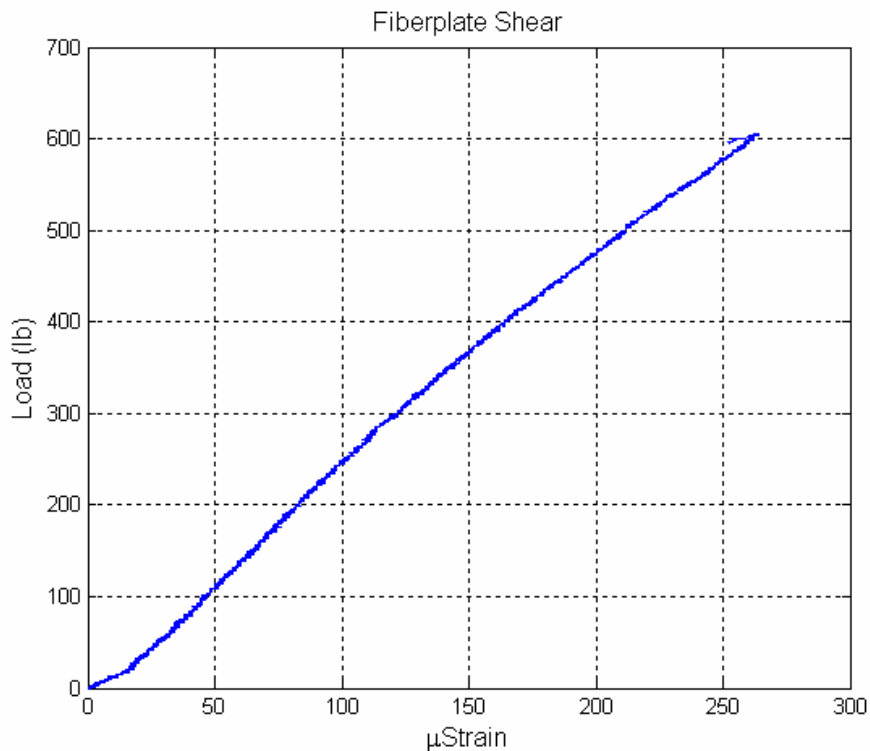


Figure 4.17 Shear Strain Values for the *Fiberplate* Configuration at the Inset of the Simply Supported Edges

The maximum shearing strain reached in the fiberplate design is 260  $\mu$ Strain. In comparison to the *tubegrate*, the shear strain values are significantly lower because of the addition of fiberglass composite top and bottom plates. It should be remembered that the square section cross members are  $\frac{1}{4}$  inch smaller, with respect to the unit dimensions, in the *fiberplate* than those in the *tubegrate*.

## Carbonplate

The *carbonplate* panel has the same geometry and design of the *fiberplate* but uses carbon fiber layers instead of fiberglass. Carbon fiber is superior to fiberglass in both weight and material properties; however, testing will determine if the benefits are greater than the cost difference.

The uniaxial gages in Figure 4.18 (a) show strain values close to those of the fiberplate. The *carbonplate's* maximum compression value (top gage) is  $-1025 \mu\text{Strain}$  and tension value (bottom gage) is  $1056 \mu\text{Strain}$ . The *carbonplate* shear strain plot is shown in Figure 4.19.

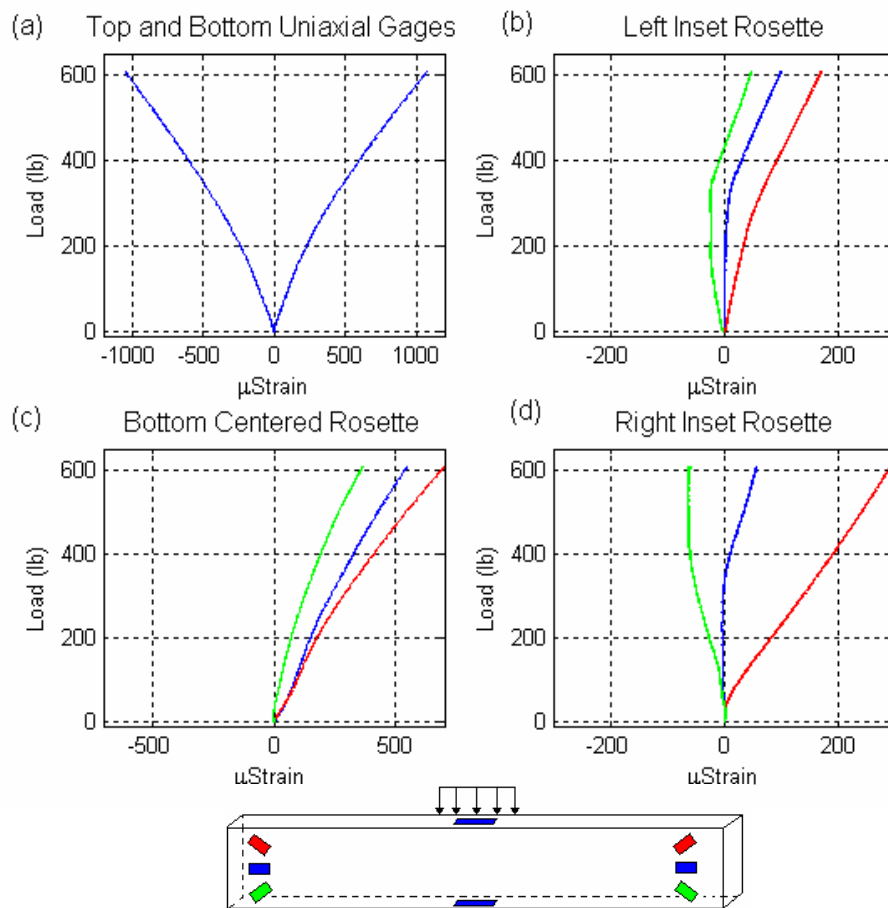


Figure 4.18 Load vs. Strain Plots of the *Carbonplate* Experimental Test

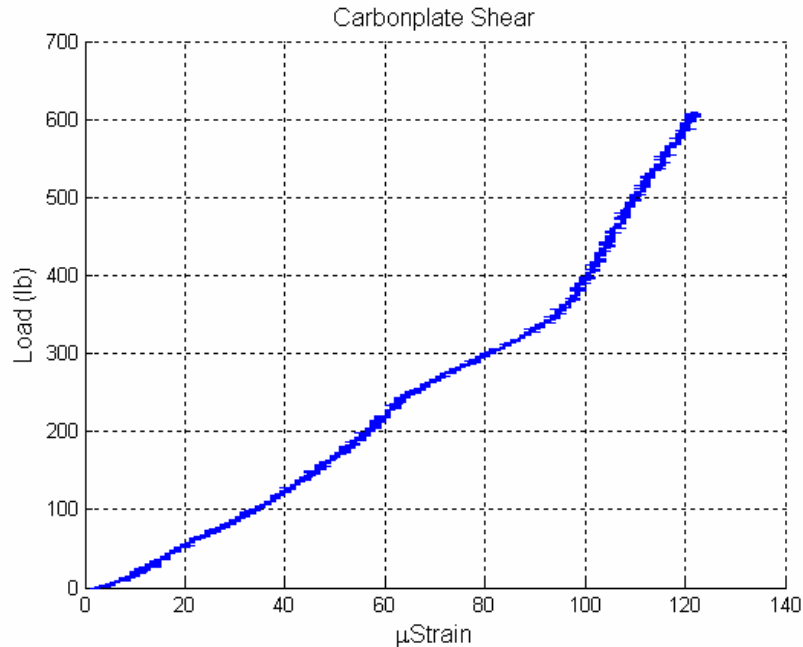


Figure 4.19 Shear Strain Values for the *Carbonplate* Panel at the Inset of the Simply Supported Edges

The shear strain in the *carbonplate* is shown in Figure 4.19. The maximum strain occurring at the 600 lb load level is 120  $\mu$ Strain. The maximum shear strain in the *carbonplate* is approximately half the maximum shear strain in the *fiberplate*. From these results, it can be stated that the carbon fiber panels which form a sandwich structure with the aluminum tubing extrusion is the most effective design for bending resistance and reduction of strain on the inset of the simply supported edges.

#### 4.5 Finite Element Modeling (ANSYS)

Finite element modeling of each panel design was performed to better understand the performance of each structure. Experimental analysis of the designs most accurately characterizes the performance of each design configuration; however, experimental testing is timely and expensive. Creating accurate finite element models will provide insight into the benefits of a design concept before the performing the manufacturing process, instrumentation, and experimental test procedures.

#### **Tubeplate**

Material: 12, 1 inch aluminum tube extruded cross members  
 Young's Modulus = 10 Msi  
 Poisson's Ratio = 0.33  
 Tube Thickness: 2/32 inch

Panel Dimensions: 1 ft x 1 ft x 1 inch

Elements: Shell

Boundary Conditions: All DOF fixed on plate edge perpendicular to cross members.

Load: 2 inch x 3 inch steel plate with a defined displacement into the panel

The geometry of the *tubeplate* was created using Pro Engineer. The process in Pro Engineer was to create the tube cross section and extrude it to the length of the plate. After one tube was created, the tube was patterned and spaced 0.001 inches apart to account for the natural gap between the adjacent surfaces. The pattern resulted in a total of twelve, 1 inch tubes butted together which yielded a panel of 12 inches by 12 inches or 1 square foot.

The Pro Engineer geometry was imported into ANSYS finite element software. The material properties and dimensions for the *tubeplate* were defined. In order to create the desired element size, the element size definition was set to 0.2" before meshing. Simulation of the weld points between tubes was done by "coupling the degrees of freedom" between adjacent nodes where the butted tubes were connected. The *Couple DOFs* command in ANSYS defines the motion/displacement of the selected nodes to be coupled together as depicted in Figure 4.20.

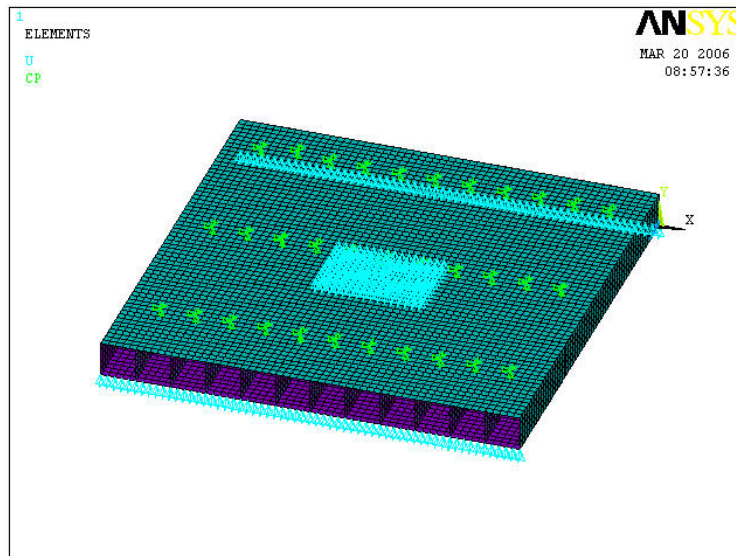


Figure 4.20 Tubeplate Finite Element Model Displaying the Boundary Conditions, Load, and Coupled Degrees of Freedom as Weld Connections

The results from the finite element modeling are used as a comparison to the displacement and recorded strain gage values from the experimental analysis. The uniaxial measurements are taken next to the load on the top and bottom of the panel. This corresponds to the x-direction strain measurement in the finite element model. Also, the shear strain is analyzed by comparing the nodal and element solutions in the location of the rosette arrangements.

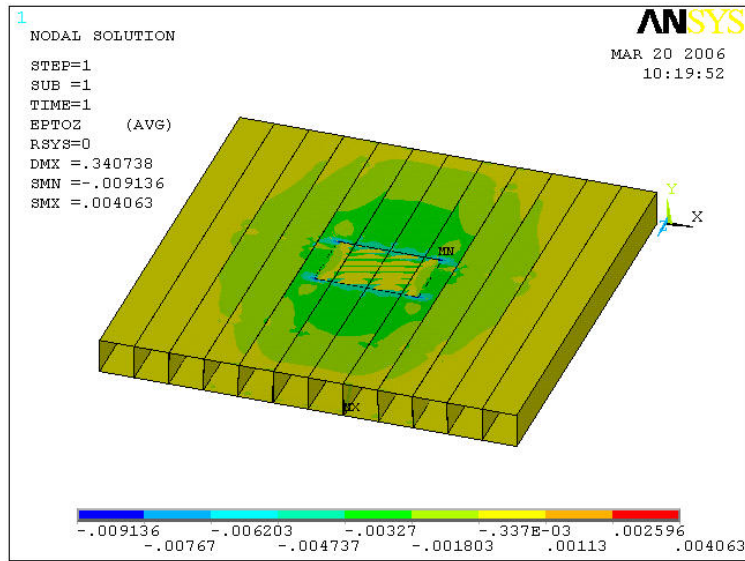


Figure 4.21 Strain in the Uniaxial Direction Corresponding to the Strain Gage Placement in the Experimental Analysis

The uniaxial strain from the *tubeplate* finite element model is shown in Figures 4.21 and 4.22. Examining the contour plots, the uniaxial strain at the location of the strain gage placements is averaged over the elements. The averaged value from the finite element model is -2033  $\mu$ Strain. The average strain values discussed in this section are attained by collecting the strain values in the elements where the strain gage has been placed for experimental analysis and averaging the results. The result for the uniaxial strain attained experimentally was -1600  $\mu$ Strain (see Figure 4.14-a).

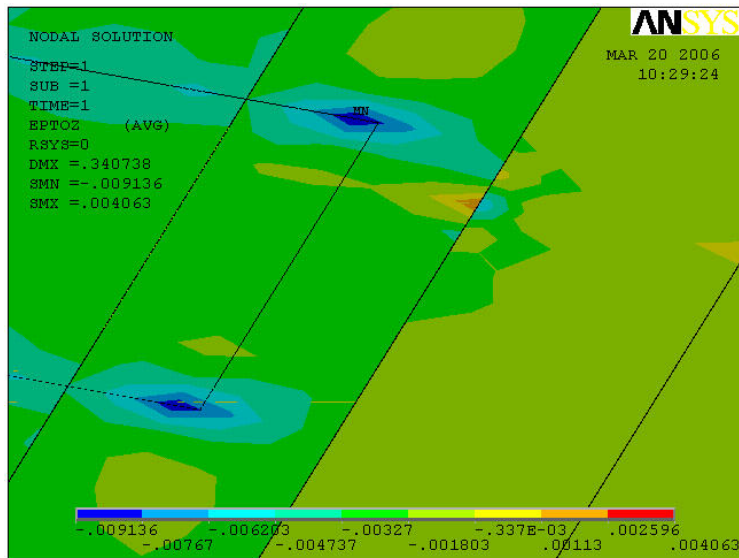


Figure 4.22 Magnified View of the Uniaxial Strain Next to the Load Area. Notice the Stress Concentration Next to the Weld Point



## Tubegrate

Material: 6, 1 inch aluminum tube extruded cross members

2, aluminum U-channels

Young's Modulus = 10 Msi

Poisson's Ratio = 0.33

Tube Thickness: 1/16 inch

Panel Dimensions: 1 ft x 1 ft x 1 inch

Elements: Shell

Boundary Conditions: All DOF fixed on U-channel edge perpendicular to cross members.

Load: 2 inch x 3 inch steel plate with a defined displacement into the panel creating contact.

Modeling of the *tubegrate* was similar to the *tubeplate* model but differed by incorporation of edge U-channels and spacing between tube cross members. The method to model the interface between the U-channels and cross members was determined by the manufacturing process. The weld points on the tubegrate are located on the top and bottom of the plate where the cross members meet the U-channel edge connections. To simulate this connection in ANSYS, the nodes located at the weld points were coupled by again using the **Couple DOFs** command. The *tubegrate* model created for theoretical analysis is depicted in Figure 4.23.

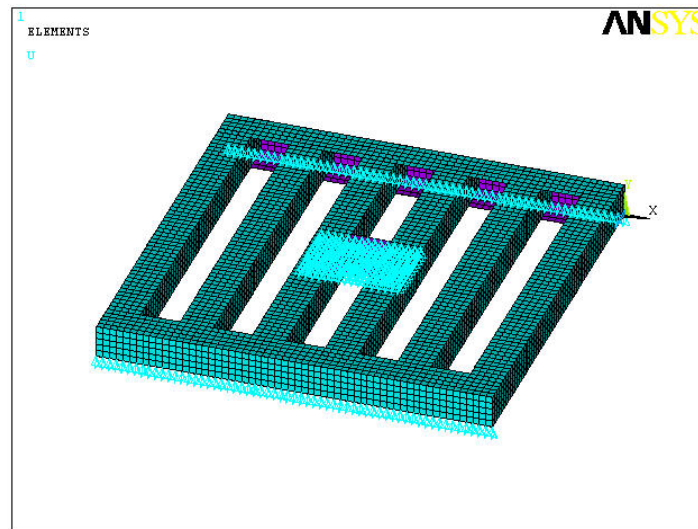


Figure 4.23 Tubegrate Finite Element Model Showing the Contact Load, Edge Restraints, and Coincident Nodes

The uniaxial strain plots are depicted in Figure 4.24. Collecting the strain data from the location of the uniaxial gages, the uniaxial strain is averaged as 5445  $\mu$ Strain. The comparative experimental value at this location is 5239  $\mu$ Strain. The top uniaxial gage, located directly under the load, experiences an experimental strain value of -4268  $\mu$ Strain. The finite element strain value at this location is -6176  $\mu$ Strain.

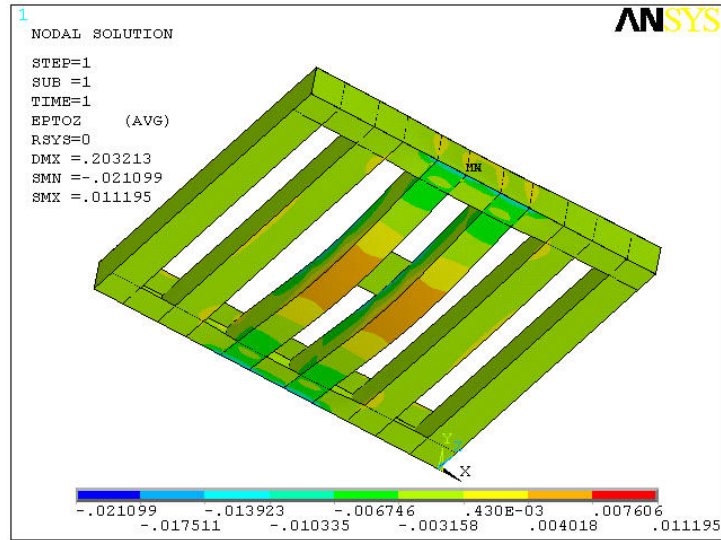


Figure 4.24 Uniaxial Strain of The Tubegrate Panel

## Fiberplate

Material: 5,  $\frac{3}{4}$  inch aluminum tube cross members

10 paper rib strips

6 aluminum sheet metal strips

12 layers of woven E-glass and epoxy fiberglass composite

Tube Thickness: 1/16 inch

Panel Dimensions: 1 ft x 1 ft x 1 inch

Elements: Shell

Boundary Conditions: Simply supported on U-channel edge perpendicular to cross members.

Load: 2 inch x 3 inch steel plate with a defined displacement into the panel creating contact.

The *fiberplate* model involved detailed finite element modeling procedures to most accurately define the panel geometry, materials, and contact characteristics. Modeling was done with shell elements containing layer definition options. Within the *fiberplate* structure, there are four different layer configurations. The layer configurations were each defined by the *shell element layer definitions* in ANSYS. The parameters defined per layer were thickness, material properties, and fiber orientation. The *fiberplate* ANSYS finite element model with boundary conditions and load application is displayed in Figure 4.25.

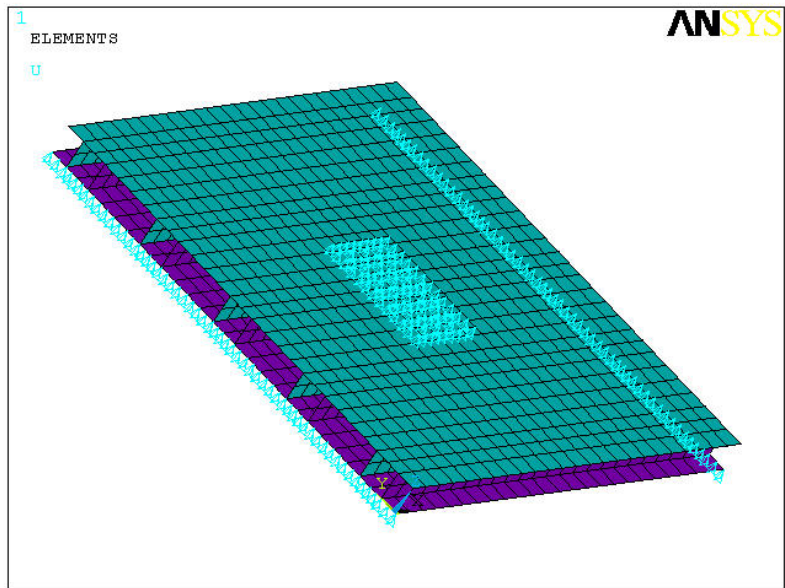
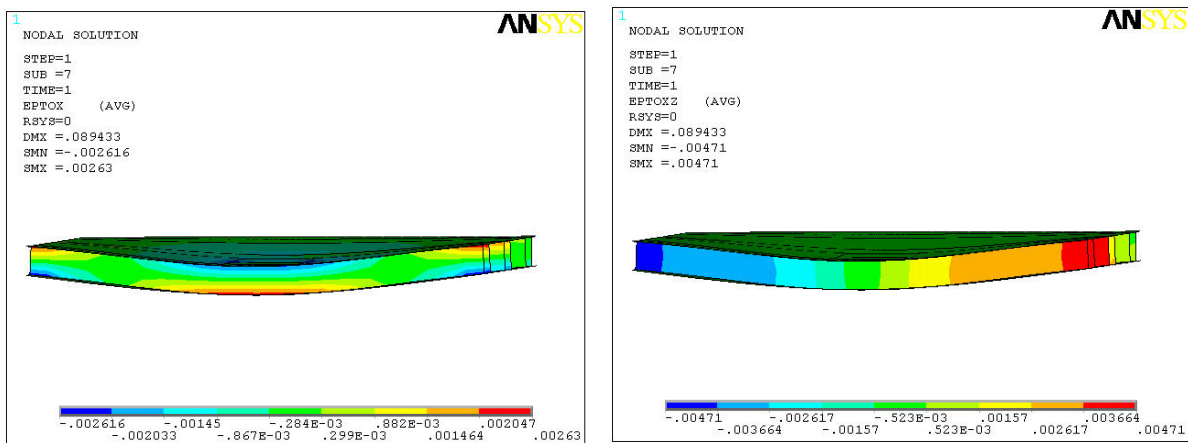


Figure 4.25 The *Fiberplate* Finite Element Model Showing the Simply Supported Edges and Load



(a) Uniaxial Strain

(b) Shear Strain

Figure 4.26 Uniaxial and Shear Strains of the *Fiberplate* Panel

The uniaxial strains in the fiberplate were predicted to be lower than those of the *tubegrate* because of the addition of the top and bottom fiberglass face sheets and the reduction in the aluminum tube cross member size. It is important to remember that each design is based on a cross section thickness of 1 inch. Therefore, in order to compensate for the face plate thickness, the cross member cross section height was reduced from 1 inch in the *tubegrate* and *tubegrate* design to 0.75 inches in the *fiberplate* and *carbonplate*.

Figure 4.26 (a) shows the *fiberplate* uniaxial strain contour plot. The averaged value of the finite element model in the region of the top uniaxial strain gage is -1732  $\mu$ Strain. The experimental value at this location is -1003  $\mu$ Strain. The bottom uniaxial gage averaged value is 1656  $\mu$ Strain and the corresponding experimental value is 1069  $\mu$ Strain.

The *fiberplate* shear strain contour plot is displayed in Figure 4.26 (b). Following the trend of comparison between theoretical and experimental values, the strains again are calculated to be of higher magnitude than the experimental results. The averaged theoretical strain is 2749  $\mu$ Strain and the corresponding experimental value is 267  $\mu$ Strain. The theoretical value is greater than the experimental by a magnitude of ten. The large difference in values can be attributed to the contact connection between the core cross members and the top and bottom face sheets. A “bonded” connection is established in the finite element model which coincides the movement of the surfaces in contact between the face sheets and the core cross members. Therefore, the compression action of the top face sheet and tension of the bottom face sheet by flexure is directly transported to the cross member creating a higher shear resultant load. These same actions are produced in the experimental procedure but slippage and ductility in the bond will lessen the magnitude of the shear strain transmitted to the core cross members.

## **Carbonplate**

Material: 5,  $\frac{3}{4}$  inch aluminum tube cross members

10 paper rib strips

6 aluminum sheet metal strips

12 layers of 2x2 twill weave graphite fabric and epoxy carbon fiber composite Tube

Thickness: 1/16 inch

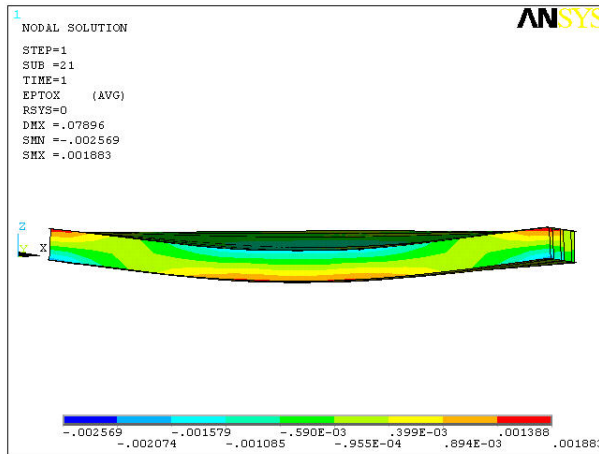
Panel Dimensions: 1 ft x 1 ft x 1 inch

Elements: Shell

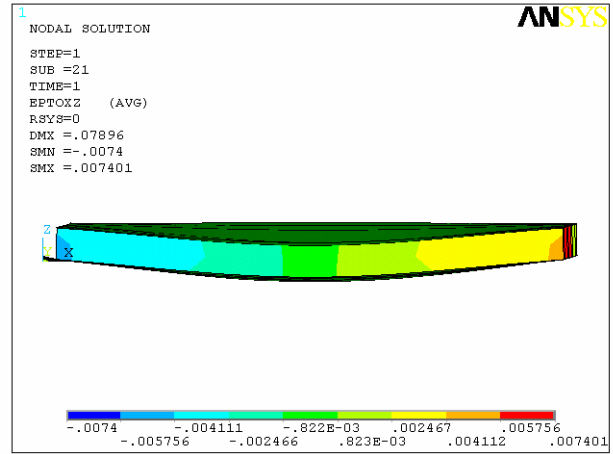
Boundary Conditions: Simply supported on U-channel edge perpendicular to cross members.

Load: 2 inch x 3 inch steel plate with a defined displacement into the panel creating contact.

The carbonplate design is identical to the fiberplate layup except carbon fiber is used in the faceplates instead of fiberglass. The impetus to use carbon as the fiber material was for maximizing the fiber material properties and weight saving characteristics. As seen in the material properties, carbon fiber is superior to fiberglass producing higher stiffness values and ultimately increasing the load carrying capabilities. The finite element uniaxial and shear strain contour plate of the *carbonplate* is displayed in Figure 4.27.



(a) Uniaxial Strain



(b) Shear Strain

Figure 4.27 Uniaxial and Shear Strains of the *Carbonplate* Panel

#### 4.6 Failure Analysis

A triaxial state of stress is developed in the panel designs during the loading procedure which initiates the use of an equivalent stress value or failure criterion to investigate the effect of material yielding. Von-Mises stress is a stress parameter that expresses the octahedral shear stress, or the strain energy of distortion, at any point within a body which undergoes a triaxial state of stress (*Chen and Han, 1987*). Von-Mises stress criteria uses the stress components at any point within the body and is expressed as:

$$S_{eq} = \sqrt{\frac{1}{2} [(\sigma_x - \sigma_y)^2 + (\sigma_y - \sigma_z)^2 + (\sigma_z - \sigma_x)^2 + 3\tau_{xy}^2 + 3\tau_{yz}^2 + 3\tau_{xz}^2]}$$

The Von-Mises failure criteria states that material yielding begins if the equivalent stress at any point reaches the material yielding point. The stress plots from the *fiberplate* and *carbonplate* designs are analyzed using the Von-Mises criteria to determine failure characteristics.

The plots of the Von-Mises stress in the *fiberplate* and *carbonplate* designs are shown in Figures 4.28 to 4.31.

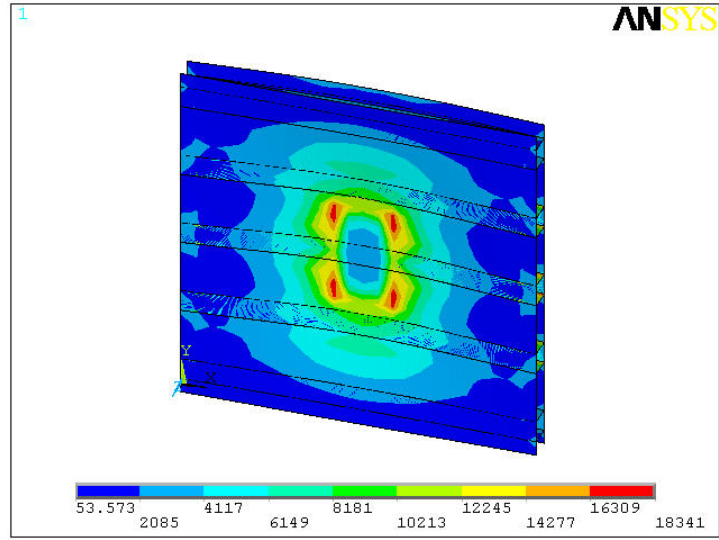


Figure 4.28 Contour Plot of Von-Mises Stress in the Fiberplate

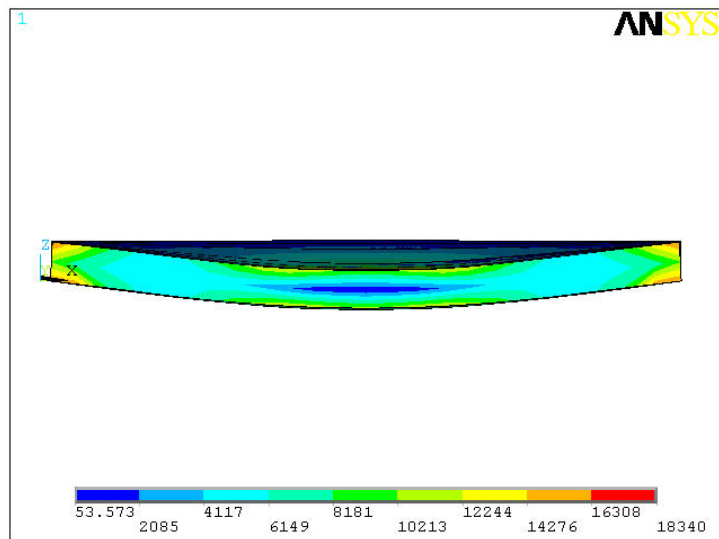


Figure 4.29 Contour Plot of the Von-Mises Stress in the Core of the Fiberplate

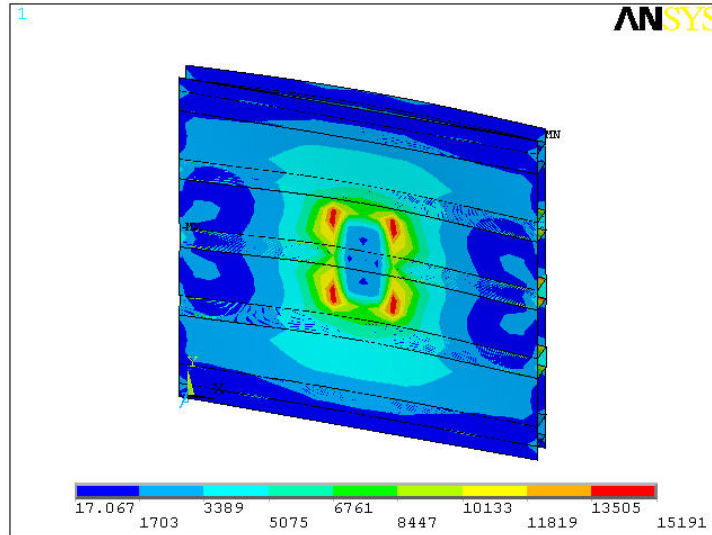


Figure 4.30 Contour Plot of the Von-Mises Stress in the Carbonplate

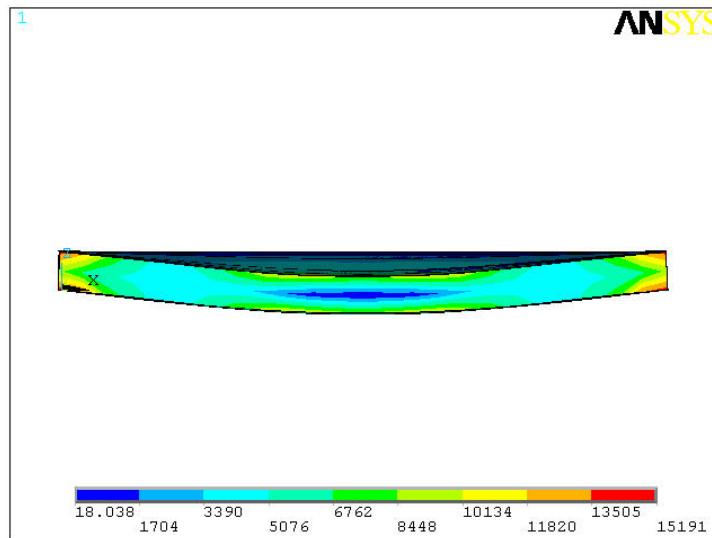


Figure 4.31 Contour Plot of the Von-Mises Stress in the Core of the Carbonplate

The Von-Mises stress values from the finite element contour plots are used to determine if there is failure in the panel core. As previously described, failure according to the Von-Mises criteria occurs when the energy of distortion (plotted values) reaches the same energy for yield/failure under uniaxial tension. The value in which yielding occurs in the aluminum core structure is 60 ksi (*Hibbeler, 2005*). The maximum values attained in the *fiberplate* and *carbonplate* designs are listed in Table 4.2.

Table 4.2 Failure Criteria for the *Fiberplate* and *Carbonplate* Core Structure

Panel Configuration	Strength of the Core Structure (ksi)	Maximum Von-Mises Stress in the Core (ksi)	Factor Of Safety
Fiberplate	60	15.3	3.92
Carbonplate	60	12.7	4.72

From Table 4.2, it is shown that the maximum Von-Mises stress values attained in the *fiberplate* and *carbonplate* designs are almost four times less than the tensile yield strength of 60 (ksi) for the aluminum core structure. Therefore, it is determined that applying a load of 600 lbs to a square foot section of the *fiberplate* or *carbonplate* design will not cause yielding within the core structure.

### Composite Failure

Failure in composite structures is often complex and involves various modes of failure. Methods of fracture of composite materials include the following.

- Fiber breaking
- Matrix Crazeing
- Matrix Cracking
- Fiber Debonding
- Delamination

It is difficult to apply all the failure modes into the design and analysis of the part. The basic approach involves using an empirical failure criterion, similar to the Von-Mises criteria previously discussed. The maximum stress criterion (*Barbero, 1998*) will most efficiently provide an understanding into the failure prediction of the *fiberplate* and *carbonplate* designs.

The maximum stress criterion for composite material analysis involves comparing the stress values attained by theoretical or experimental analysis to the strength values of a single laminate layer within the composite structure. The criterion predicts failure of a layer when one of the stresses in material coordinates  $(\sigma_1, \sigma_2, \sigma_6, \sigma_4, \sigma_5)$  exceeds the layer strength. The criterion states that failure will occur if any of the following parameters are true

$$\sigma_1 > F_{1t} \quad \text{if } \sigma_1 > 0$$

$$|\sigma_1| > F_{1c} \quad \text{if } \sigma_1 < 0$$

$$\sigma_2 > F_{2t} \quad \text{if } \sigma_2 > 0$$

$$|\sigma_2| > F_{2c} \quad \text{if } \sigma_2 < 0$$

$$|\sigma_4| > F_4$$

$$|\sigma_5| > F_5$$

$$|\sigma_6| > F_6$$

where



- $F_{1t}$  – tensile strength in the fiber direction
- $F_{1c}$  – compressive strength in the fiber direction
- $F_{2t}$  – tensile strength in the transverse direction
- $F_{2c}$  – compressive strength in the transverse direction
- $F_6$  – inplane shear strength
- $F_4, F_5$  – interlaminar shear strength values

The comparison of the determined stress values to the strength values of single laminate layer will determine if failure is reached in the composite structure. Tables 4.3 and 4.4 present the results of the maximum stress criterion for the *fiberplate* and *carbonplate* composite structures.

Table 4.3 *Fiberplate* Maximum Stress Criterion

Strength Parameter	Fiberplate Strength Values (ksi)	Corresponding Stress Values (ksi)	Factor Of Safety
$F_{1t}$	53.0	14.7	3.61
$F_{1c}$	79.6	21.0	3.80
$F_{2t}$	53.2	11.0	4.84
$F_{2c}$	79.6	14.7	5.41
$F_6$	14.1	1.65	8.55

Table 4.4 *Carbonplate* Maximum Stress Criterion

Strength Parameter	Carbonplate Strength Values (ksi)	Corresponding Stress Values (ksi)	Factor Of Safety
$F_{1t}$	80	11.4	7.01
$F_{1c}$	113	12.9	8.76
$F_{2t}$	82.5	8.0	10.3
$F_{2c}$	98.6	10.3	9.57
$F_6$	14.2	1.52	9.34

The previous tables show that the lowest factor of safety attained for the *fiberplate* composite structure is 3.61 and the *carbonplate* structure is 7.01. The determined factors of safety determine that the composite structure within each design will not fail when loaded with a 600 lb load per square foot section.

It should also be stated that if a 600 lb/ft<sup>2</sup> load is applied as the load on the floor of a 54 ft. trailer platform, the overall trailer cargo load would equal 129,600 lbs or approximately 65 ton. The average payload capacity is 25 ton per cargo load. Therefore, a 2.5 factor of safety is included in the applied load.

## 4.7 Discussion

As shown in the four panel comparative study, there are four options of progressive design, meaning, each design was upgraded or altered from the previous. The designs progressed to efficient load bearing platforms with weight saving properties. The objective of this study was to create weight efficient platform to initiate in heavy vehicle applications or any application in which lightweight and strength characteristics are desired and mandatory. Table 4.5 lists the four panel designs and their respective weights versus the square foot section of an existing trailer section.

Table 4.5 Weight of Panel Designs Compared to an Existing Trailer Section

Panel Design	Weight of Square Foot Section (lbs)
Tubeplate	3.4
Tubeplate	2.6
Fiberplate	2.4
Carbonplate	2.2
Existing Trailer Section	21.6

In Table 4.5, the cross section thickness of the sandwich panel designs is one inch and the highest weight savings is exhibited in the *carbonplate* design, with a weight saving capability of approximately 10 times less than the existing current trailer section. The other panel designs also display promising weight saving abilities. The least efficient design is the *tubeplate*, which has a weight per square foot value of 3.4 lbs. Even as the heaviest panel design, the *tubeplate* contributes a weight savings of 18.2 lbs per square foot versus the existing trailer section.

The weight comparison of Table 4.5 presents extraordinary weight efficient characteristics of the panel designs. However, the existing trailer section is composed of four inch steel I-beams and a 1 3/8 inch solid oak platform connected to the top flange. It is not expected that the one inch panel sections will compare to the current trailer section on the basis of bending resistance and load carrying capabilities. Increasing the panel dimensions to attain a four inch cross section thickness and comparing to the existing trailer section will reveal if the designs are beneficial in comparison to a trailer platform.

A final comparative finite element study was performed. The study involves the *carbonplate* design and a model of the existing trailer section. The *carbonplate* thickness and dimensions have been increased to create a four inch cross section thickness and will be noted as *carbonplate-4*. The goal is to determine if the maximum displacement and strain values of the *carbonplate-4* panel will be less than the existing trailer design of four inch steel I-beams and 1 3/8 inch solid oak platform. The following finite element models of the *carbonplate-4* and existing trailer section are shown in Figure 4.32.

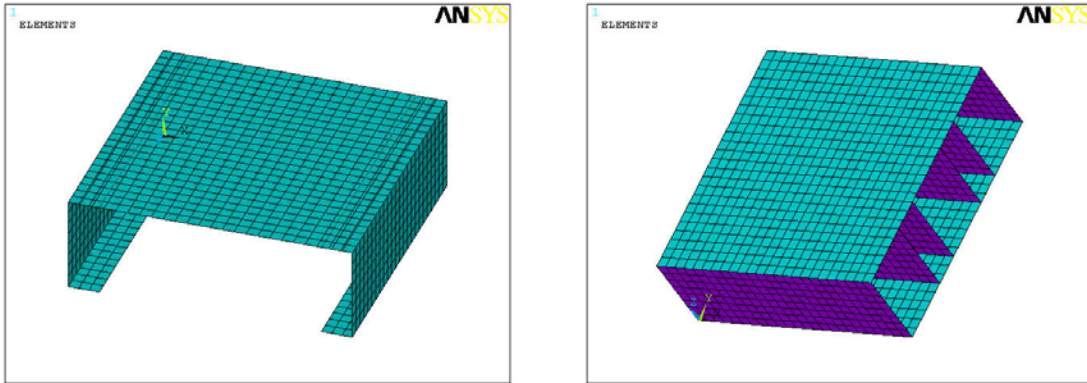


Figure 4.32 Finite Element Models of the Trailer Section and the Carbonplate

After applying the same distributed load to each model the displacements were analyzed. Figures 4.33 and 4.34 illustrate the displacement contour plots for the trailer section and the comparative *carbonplate-4* model, respectively. It is seen that the maximum displacement of trailer section is  $0.737 \times 10^{-3}$  inches. The maximum displacement in the *carbonplate-4* is  $0.104 \times 10^{-3}$  inches; this value is more than seven times less than the maximum displacement of the existing trailer section.

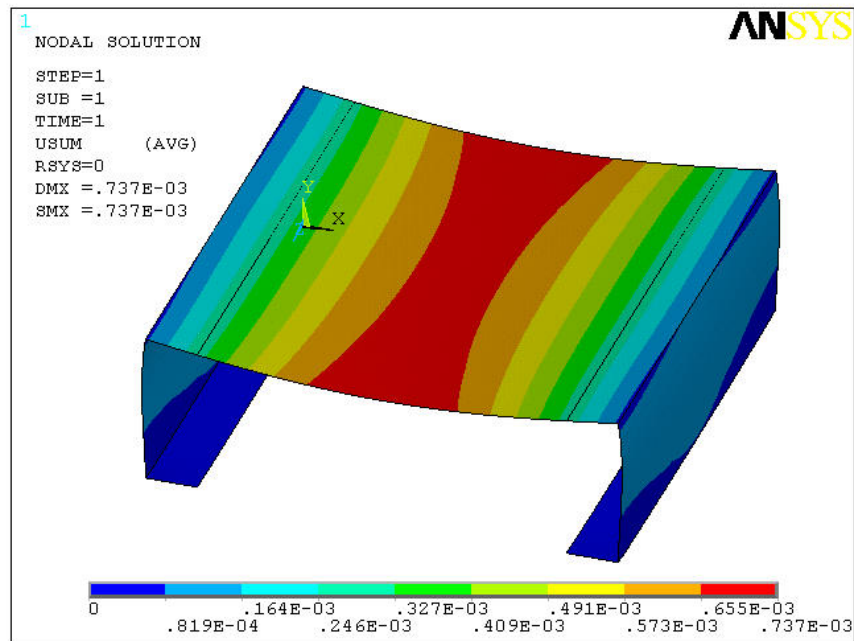


Figure 4.33 Displacement Contour Plot of the Trailer Section Model

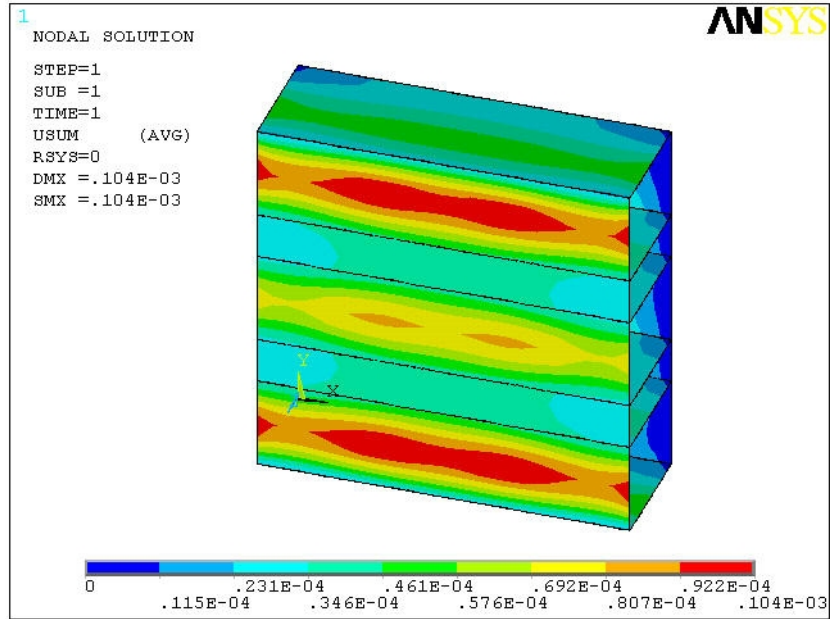


Figure 4.34 Displacement contour Plot of the Carbonplate-4 Section

The shear strains of each model can also be studied and compared. The maximum shear strain occurring in the trailer section is 37  $\mu$ Strain and is shown in the contour shear strain plot of Figure 4.35.

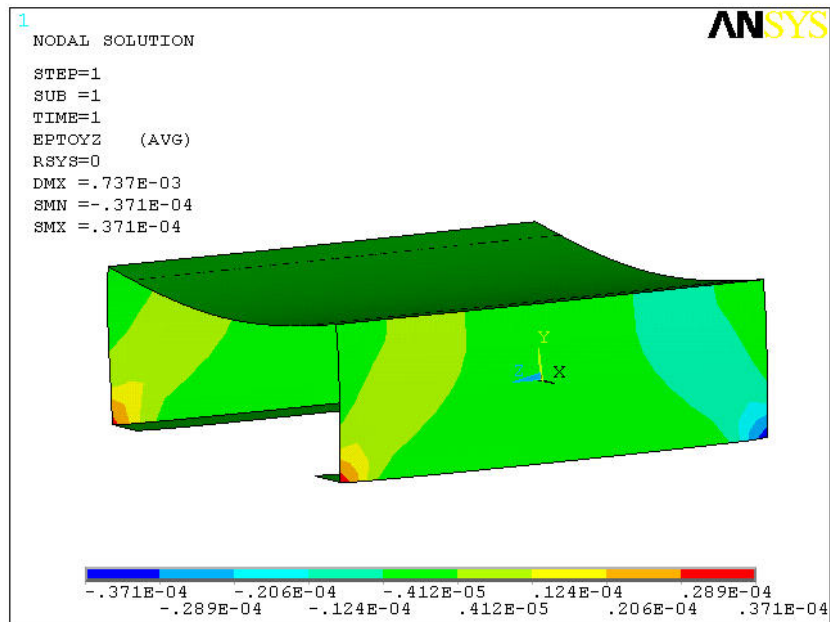


Figure 4.35 Shear Strain Contour Plot of the Trailer Section Model

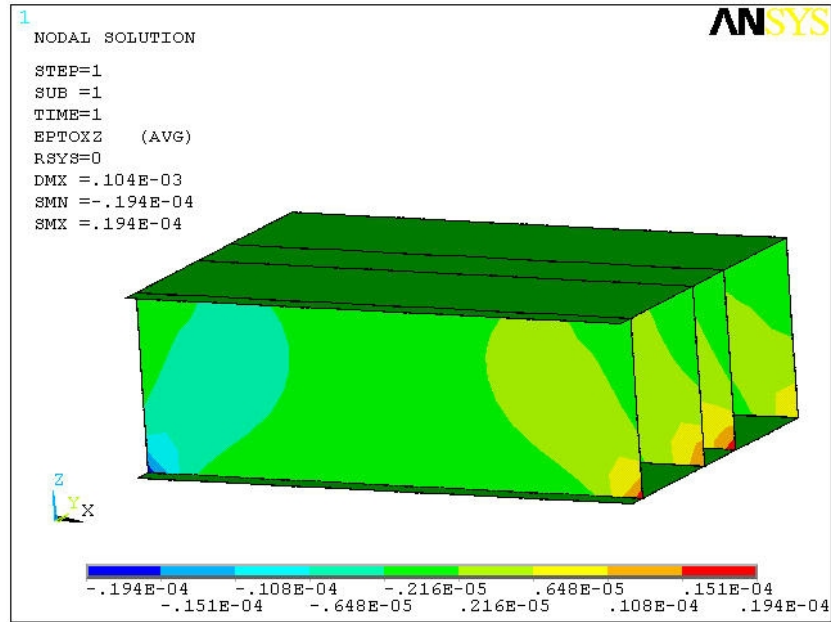


Figure 4.36 Shear Strain Contour Plot of the carbonplate-4 Model

In comparison to Figure 4.35, the maximum shearing strain in the *carbonplate-4* is 19  $\mu$ Strain. As seen in Figure 4.36, the bottom corners of the center core cross member are the location of the maximum shear strain. Comparing the maximum strain values of each model reveals the trailer section has a shear strain value of approximately two times the *carbonplate-4* model.

The square foot weight of the *carbonplate-4* panel is 7.0 lbs. If the I-beams and oak floor were replaced with the *carbonplate-4* design, the weight savings per square foot would be 14.6 lbs which correlates to a total of 6,307.2 lbs saved for a 54 ft. trailer haul. This figure can be maximized by creating the panel thickness which exactly matches the displacements and strains of the current existing trailer. The thickness of this structure would occur in the range between one and four inches. Also, an option to lower the cost of outfitting a 54 or 48 ft. trailer floor with the *carbonplate-4* would be to use fiberglass as the faceplate material.

A fiberglass model with a four inch cross section, *fiberplate-4*, was created to determine if the load bearing capabilities are also superior to the existing trailer design and comparable to the *carbonplate-4* panel. The reaction contour plots for the *fiberglass-4* panel are shown in the following figures.

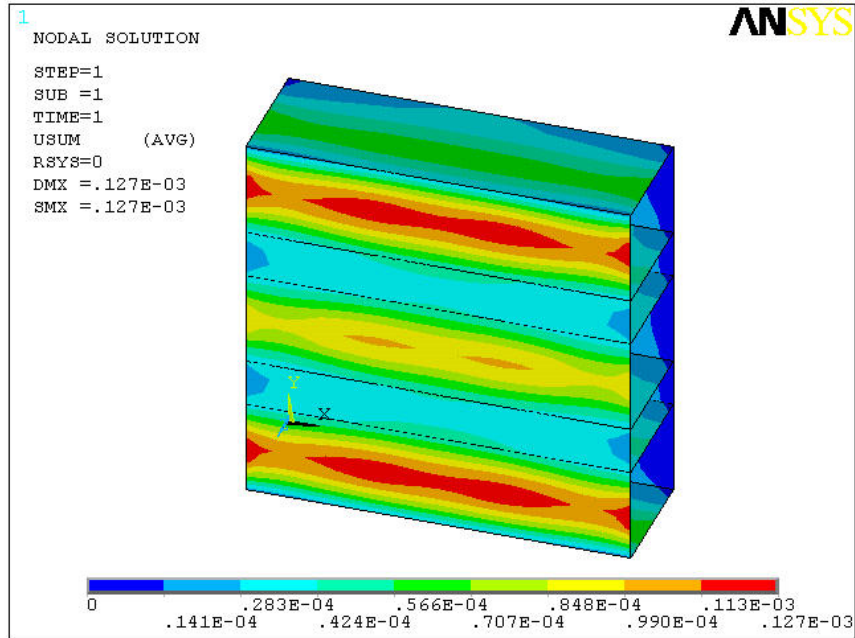


Figure 4.37 Displacement Contour Plot of the Fiberglass-4 Model

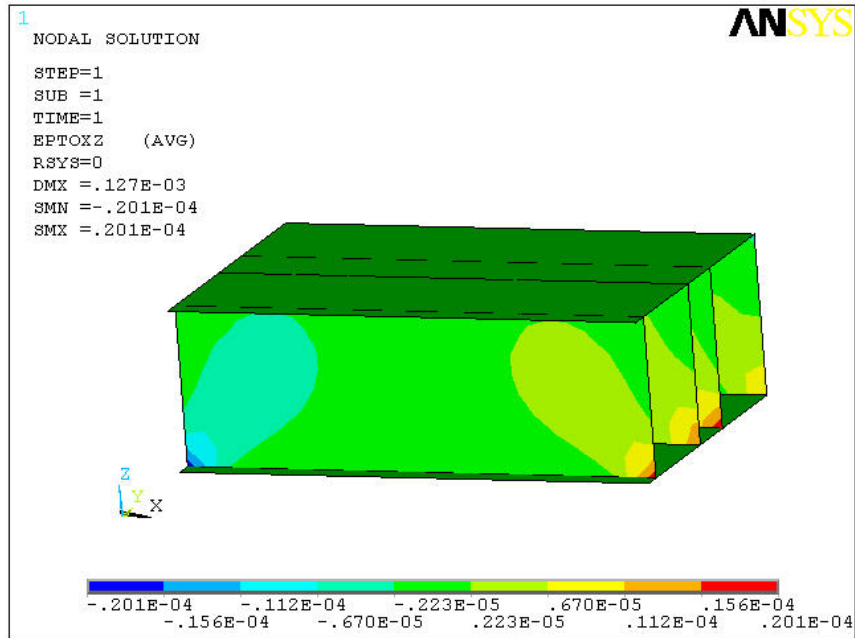


Figure 4.38 Shear Strain Contour Plot of the Fiberglass-4 Model

The displacement and shear strain of the *fiberplate-4* model are shown in Figures 4.37 and 4.38, respectively. The displacement and strain values are both superior to those of the trailer section, Figures 4.35 and 4.36. The maximum displacement is  $0.127 \times 10^{-3}$  inches and the

maximum shear strain is 20  $\mu$ Strain. Therefore, the fiberglass design is also an option to replace the existing current floor structure of steel I-beams and solid oak covering. The weight of the *fiberplate-4* panel per square foot is 7.206 lbs and is slightly heavier than the *carbonplate-4* design. The total weight savings for a 54 ft. trailer floor using the *fiberplate-4* design is 6,218.2 lbs. The weight savings for both the carbon fiber and fiberglass designs are extremely significant. The carbon fiber design is superior for weight savings and load bearing capabilities, however, taking into account the slight margin of difference in performance and the cost of carbon fiber to fiberglass, equipping the trailer floors with a lower cost fiberglass design and sacrificing small weight and stiffness penalties may result in the most practical alternative.

## CHAPTER FIVE

### IMPACT AND FLEXURAL TESTING ON SANDWICH PANELS

#### 5.1 Introduction

The research work conducted at WVU focused on investigating the potential benefits and barriers of using sandwich panels for selected for the sides of heavy trailers. For this purpose, sandwich panel specimens constructed from faceplates made out of different materials and epoxy core were made. The specimen dimensions were selected to be 4"× 4"× ¼". Loctite Hysol 4550 epoxy was selected as a core material. Three specimen lay-up configurations were considered in this study as illustrated in Table 5.1. Each specimen configuration was tested under impact and flexure.

Table 5.1 Specimen Lay-up Configuration

Specimen	Lay-up
1	16ga Steel / epoxy / 22ga Steel
2	16ga Steel / epoxy / 22ga Steel
3	16ga Steel / epoxy- carbon fiber / 22ga Steel

#### 5.2 Impact Testing

Three impact tests were performed to test the capabilities of each sandwich panel configuration. The testing procedures consisted of the following steps.

1. The test specimen was mounted to a solid frame so that only the panel resists the impact energy. The specimen was mounted to the frame in such a way that the thickest steel side is receiving the impact.
2. A testing ground was fixed and the distance from the firing point to impact point of the panel was measured. The test distance was set at 60 ft.
3. Practice shots were performed to ensure the accuracy of the firearm.
4. Test specimen was placed at marked location.
5. Panel was fired at and impacted.

Table 5.2 presents the specifications of the firearms and the bullet weights used in different impact tests.



Table 5.2 Specifications of Firearm and Bullet Weights

Test	Panel	Firearm	Bullet Weight (grains)
1	1	30.06 Rifle	180
2	2	0.22 Rifle	40
3	3	9 mm Handgun	124

Table 5.3 lists specifications for common cartridges and rifles. The three firearms used in the impact testing were the 0.22 rifle, 30.06 rifle and 9 mm handgun.

Table 5.3 Specifications of Riffls and Cartridges

Cartridge	Bullet Weight (grains)	Muzzle Velocity (ft/s)	100 yard Velocity (ft/s)	100 yard Kinetic Energy (ft-1b)	100 yd Taylor Index
0.22 Rifle	40	1150	976	85	1.2
223 Rem.	53	3330	2865	966	4.9
9 mm Tan.	124	1400	1000	250	N/A
7mm Rem.	154	3200	2966	3008	18.5
308 Win	150	2820	2593	2239	17.1
30.06	180	2700	2484	2466	19.7
416 Rigby	400	2400	2184	4236	51.9
450 Marlin	350	2100	1710	2272	39.2
470 N.E.	500	2150	1907	4037	64.6
50 BMG	750	2769	2681	11965	146.5

The bullet velocity can be interpolated for the distance used in the test and therefore the kinetic energy before impact can be determined from the Equation:

$$K.E. = \frac{1}{2}mv^2 = \frac{W v^2}{450436} \dots\dots\dots (1)$$

Where

- KE = Kinetic energy, ft-lbs
- m = Bullet mass, slugs
- v = Bullet velocity, ft/s
- w = Bullet weight, grains

Table 5.4 Data for Test Parameters

Cartridge	Bullet Weight (Grains)	20 yard Velocity (ft/s)	20 yd. Kinetic Energy (ft-lb)
0.22 Rifle	40	1115	110.4
30.06 Rifle	180	2657	2821.0
9mm Handgun	124	1200	396.5

The first panel was impacted with the 30.06 caliber rifle and was fully penetrated as shown in Figure 5.1-a. This was expected for the high energy (2821 ft-lb) being distributed over the minimal bullet projection area. The second panel was not penetrated when it was impacted with the 0.22 caliber rifle as depicted in Figure 5.1-b. The impact energy was high (110.4 ft-lb) but a large degree less than 30.06 rifle. The two test panels were manufactured with the same lay-up and were replicated as close as possible for hand manufacturing. By holding the

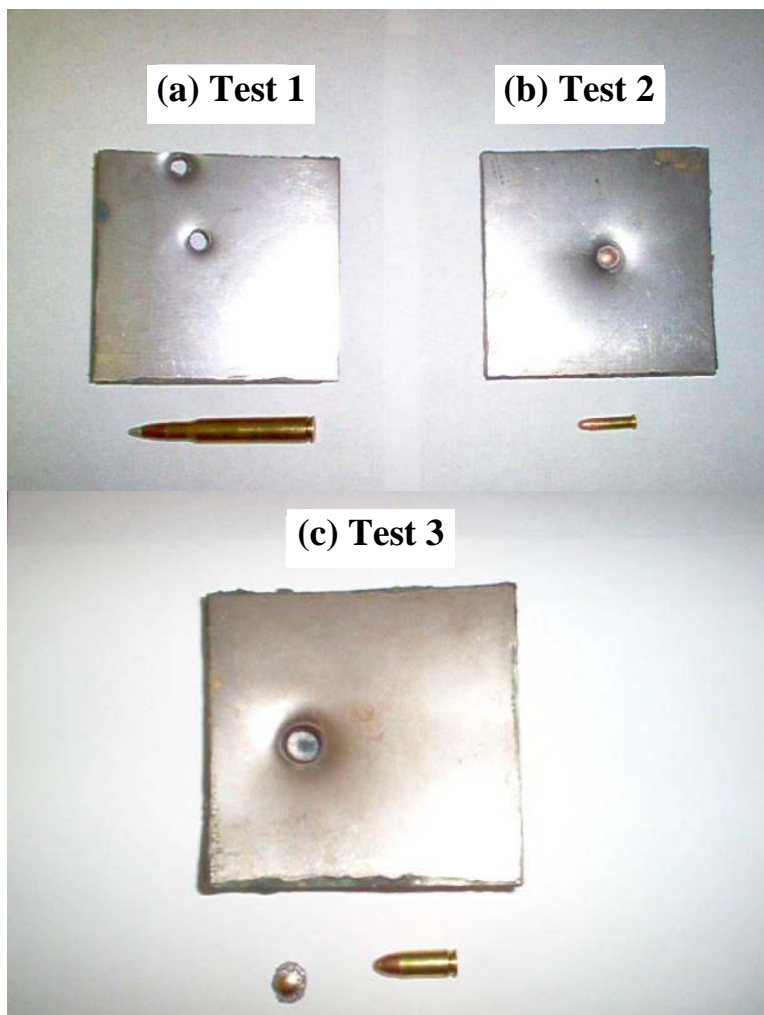


Figure 5.1 Failure Modes under Different Bullet Impacts

configuration of the panels and the test parameters constant, the impact energies can be compared. This yields a range of energy within which the panel can be penetrated by a bullet. This range between the impact energy the panel will absorb without penetration and the energy it will fail under. This energy range is going to decrease by performing more tests with energies between 110.4 and 2821 ft-lbs.

After the first two impact tests, the panel configuration was reviewed and different layup configurations were studied to maximize the amount of impact energy the panel can resist. The ideas that followed were to utilize the stiffness and lightweight properties of carbon fibers into the epoxy core of the specimen. Chopped carbon fibers were mixed with the epoxy core of the specimen during the manufacturing process. The chopped carbon fibers occupied 8% of the sandwich core volume fraction. This layup configuration was tested with impact energy of 396.5 ft-lb (Test 3). The introduction of the carbon fibers into the core epoxy proved to be effective in resisting the impact load.

Improving the design or ultimately increasing the impact energy relating to panel penetration is currently being studied. These concepts will be tested and compared to the test results analyzed in this report.

### 5.3 Future Panel Configurations

The next panel configuration to be tested will include kevlar fabric in the core of the panel. Kevlar is a material with effective properties to resist impact and abrasion loading. These panel configurations will test the feasibility of implementing the impact resistant layer into the core of the specimen. The panel layup and kevlar layer can be seen in Figure 5.2.

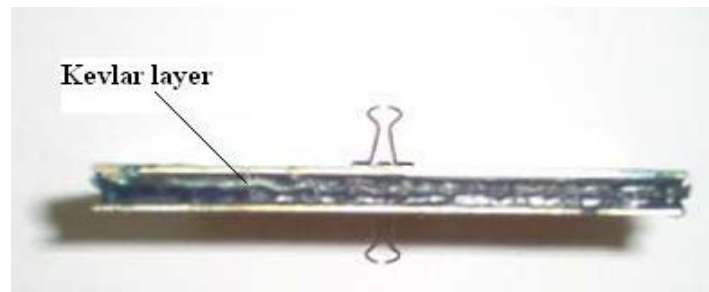


Figure 5.2 Specimen Configuration with Kevlar/Epoxy Core

Impact testing of the kevlar and epoxy core layup will reveal the impact properties of the panel and also provide information into minimizing the thickness and weight of the panel without sacrificing impact and stiffness properties. The panel specifications for impact tests four and five are listed in Table 5.5.

Table 5.5 Specimen Lay-up Configuration

Specimen	Layup
4	16ga Steel / epoxy / kevlar / epoxy / 22ga Steel
5	16ga Steel / epoxy / kevlar / epoxy / 22ga Steel

Test four will be performed with the 9mm handgun (396.5 ft-lb) and if the test is successful in resisting the impact load, then test five will be performed at a higher impact energy.

#### 5.4 Flexural Testing

This section presents the results of the three-point bending tests on sandwich panel specimens with different configurations. Two tests were conducted on each configuration design and the results of the two tests were compared and averaged. The three-point bending testing setup used in this study is shown in Figure 5.3.

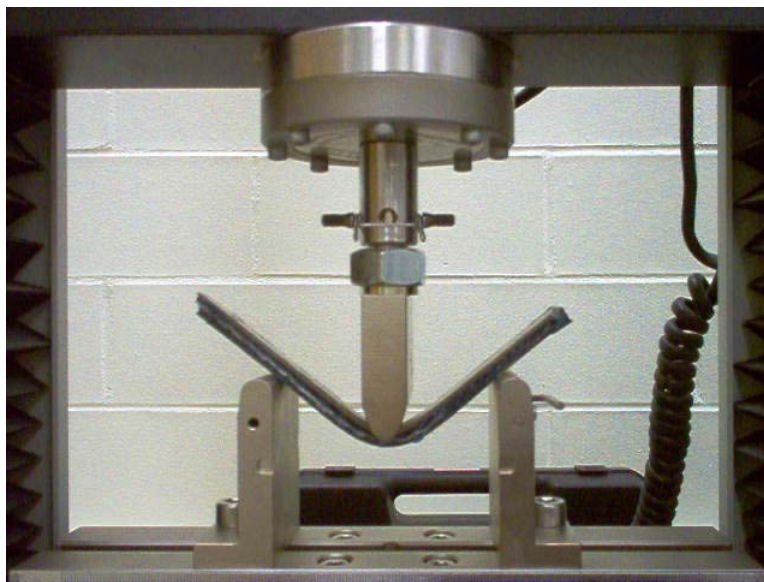


Figure 5.3 Three-Point Bending Testing Setup

The first testing was performed on Aluminum face plates and epoxy core sandwich specimens. Both face plates were identical in thickness and material characteristics. The measured load-displacement relation is shown in Figure 5.4.

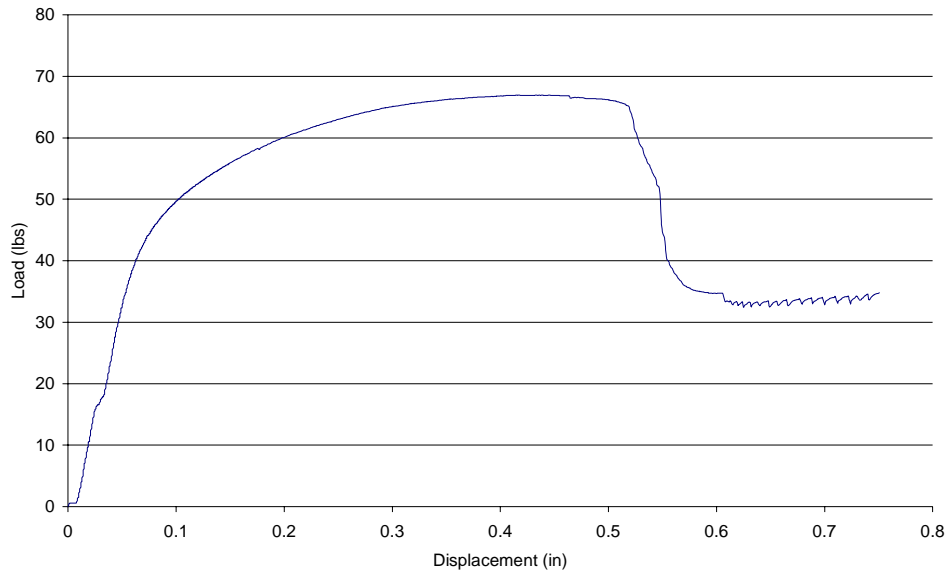


Figure 5.4 Load-Displacement Relation for Aluminum and Epoxy Sandwich Panel

The second test was for a steel and epoxy sandwich panel. The only difference for this specimen is the face sheets are a 20 gage mild steel. The epoxy and dimensions remain constant to the previous test. Figure 5.5 shows the measured load-displacement relation.

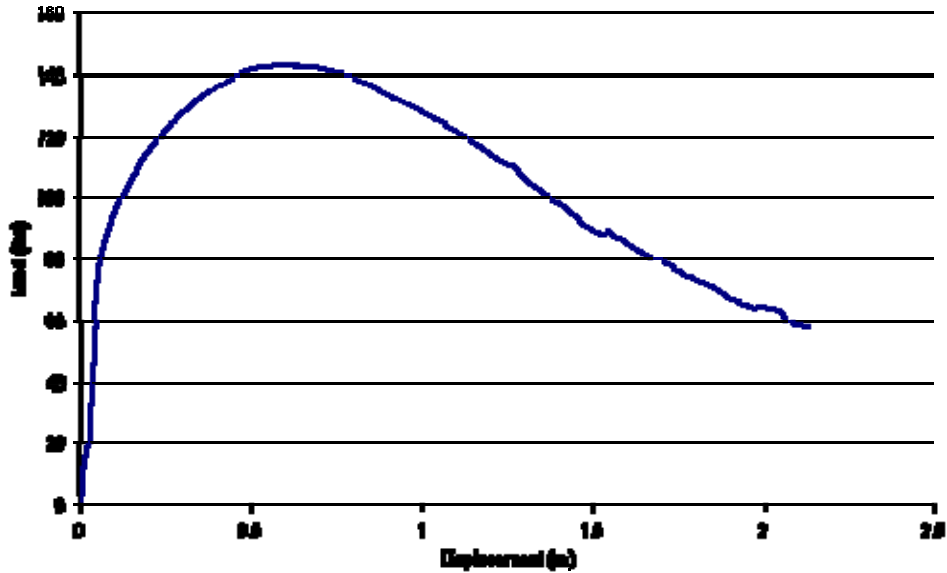


Figure 5.5 Load-Displacement Relation for 20 Gage Steel and Epoxy Sandwich Panel

The steel and epoxy construction differed from the aluminum and epoxy by the face sheets being of a different material and also thickness. This difference resulted in a significant difference in the vertical displacement and the stiffness as can be seen in Figures 5.4 and 5.5.

In van-trailers, the inner are more susceptible to impact from fork lift or other disturbances. Therefore, sandwich panels were made of face plates of different thickness. Relating to the trailer design, the thicker sheet will be inside the cargo haul to receive the impact. The outside face sheet is 20 gage mild steel and the inner sheet is a thicker 16 gage mild steel. Figure 6 illustrates the measured load-displacement relation.

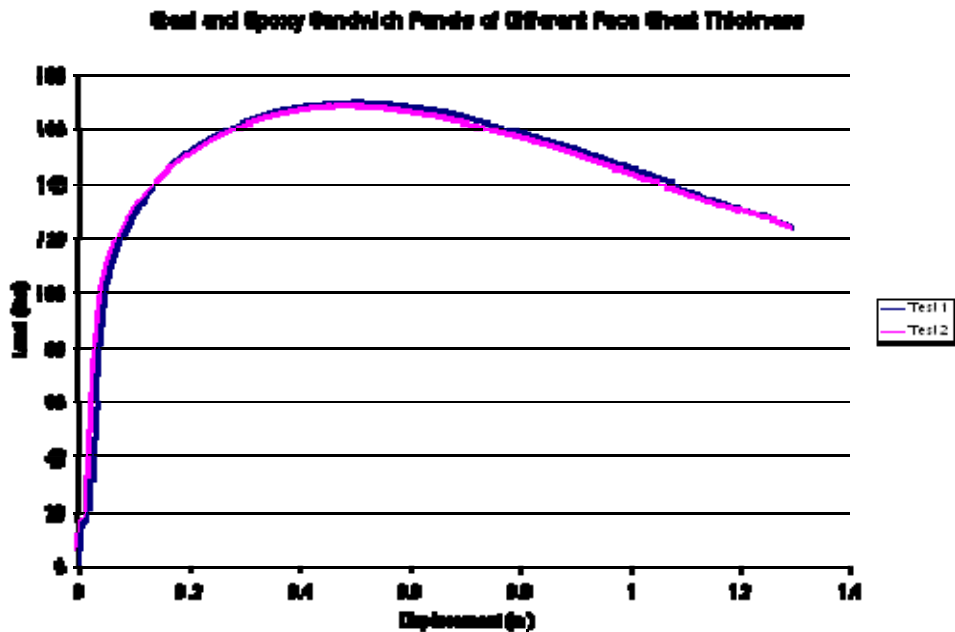
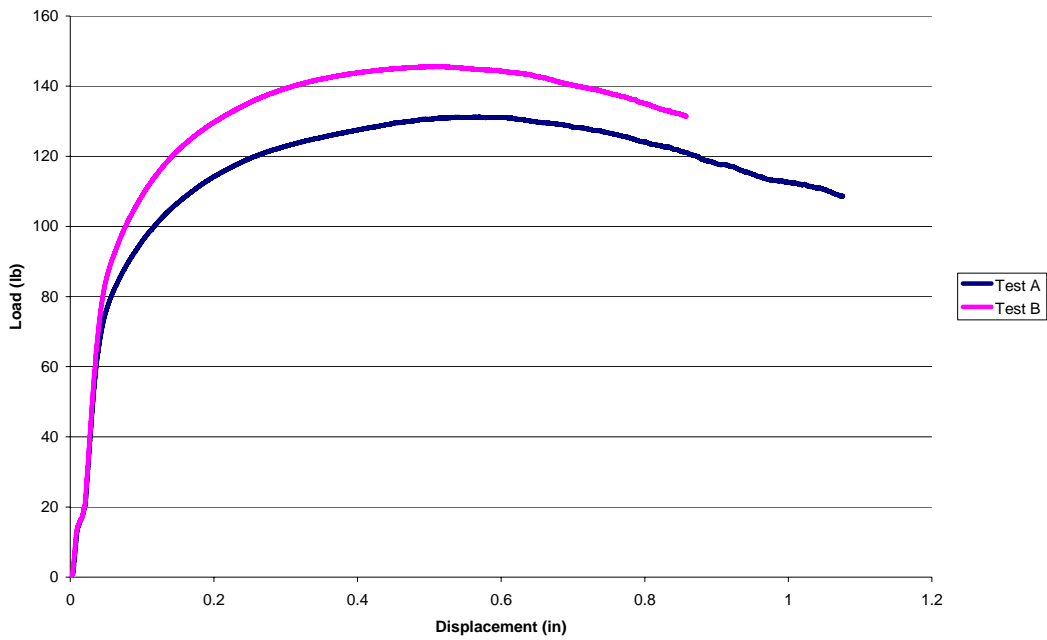


Figure 5.6 Load-Displacement Relation for Steel and Epoxy Sandwich Panel of Different face sheet Thickness

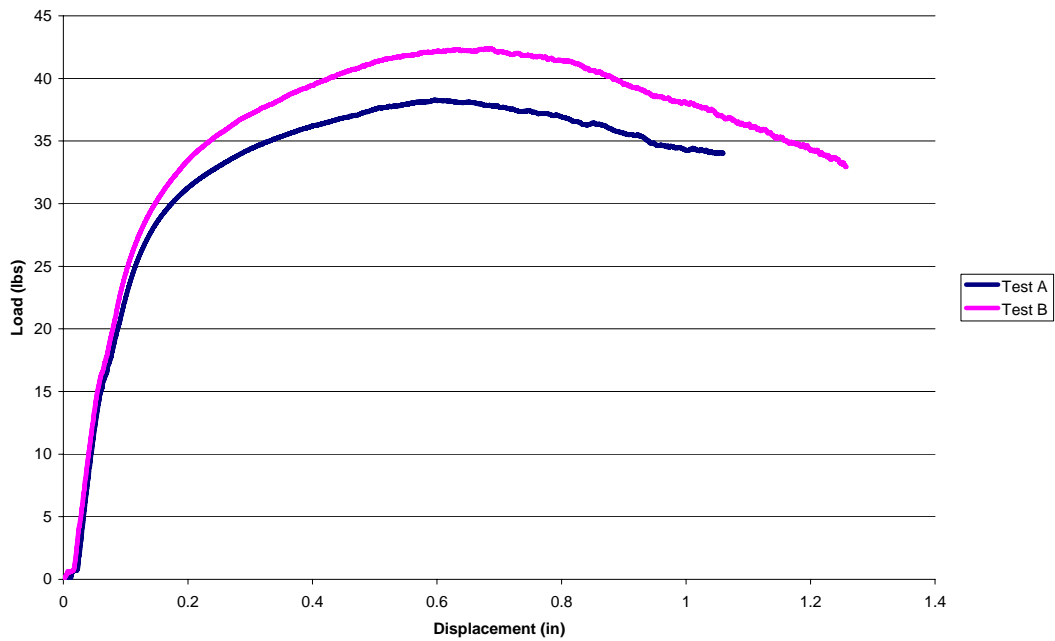
Attempts were made to reinforce the epoxy core material with different materials to examine how such a reinforcement affect the performance of the sandwich structure. For this reason, sandwich panel specimens with configurations listed in Table 5.6 were constructed and tested in bending. The results for the four three-point bending tests are displayed in Figure 5.7. The carbon fiber and epoxy panels, Figure 5.7-a, were effective in resisting the flexural load applied in the test. The kevlar and epoxy panels, Figure 5.7-b, were not as effective in resistance to bending, however, testing of their impact properties is expected to reveal a higher impact resistance than the carbon and epoxy panels.

The kevlar and epoxy panels carried approximately a third of the load that the carbon and epoxy panels sustained. This result is attributed to the higher stiffness value of the carbon fibers and also to the debonding effect that occurred on the kevlar and epoxy interface. The issue of debonding in this type of layup will be addressed by critiquing the manufacturing techniques and

also adjusting the layup configuration to place the kevlar layer where debonding will be less likely to occur.



(a) Steel with Carbon Fiber Strands and Epoxy Core.



(b) Steel with Kevlar and Epoxy Core.

Figure 5.7 Results of Three-Point Bending Tests on Sandwich Panels

Table 5.6 Specimen Lay-up Configuration

<b>Panel Type</b>	<b>Test</b>	<b>Layup</b>
1	A	16ga Steel / epoxy- carbon fiber / 22ga Steel
	B	16ga Steel / epoxy- carbon fiber / 22ga Steel
2	A	16ga Steel / epoxy / kevlar / epoxy / 22ga Steel
	B	16ga Steel / epoxy / kevlar / epoxy / 22ga Steel



## CHAPTER SIX

### CONCLUSIONS

The *carbonplate* and *fiberplate* design is a technology geared toward flooring applications in large trailer systems but can be applied to platforms or load carrying structures. In applications such as the aerospace industry and shipping industry where weight saving is crucial to the performance of the structure, composite sandwich technology with a load-bearing core structure, as shown in this work, is a promising solution. The particular composite sandwich structure studied in this work is revolutionary because it combines a core material which contributes to the bending stiffness as compared to a common sandwich structure with a core material of honeycomb, wood, or foam which do not contribute to bending resistance alone.. The bonding and joining issues of a metallic core and fiber reinforced polymer faceplates has been solved by the combination of panel geometry and adhesive bonding. The application of applying composite material technology to the entire trailer structure has been tested by the manufacturing of a scaled trailer model.

Additional conclusions which can be drawn from this work are as follows:

- Joining concepts between composite parts within a trailer system have been addressed by the construction of a trailer model and study of various joint designs. Adhesive bonding assisted by mating geometry is a method to join structures without the use of mechanical joints such as bolts or rivets.
- If replacement of the steel I-beams and oak flooring in an existing trailer is not acceptable within the trucking industry, an alternative arrangement of replacing the oak flooring alone with the *fiberplate* or *carbonplate* designs will also create respectable weight savings. The one-inch thick cross section panels will serve this design purpose.
- The *fiberplate* and *carbonplate* designs were created with the objective of designing and manufacturing a sandwich composite structure with a core material that contributes to the bending stiffness. In theory, a sandwich composite is generally composed of a honeycomb, foam, or wood core. These core materials do not contribute to bending resistance. To create this type of design, issues of bonding between the faceplates and core had to be addressed. Developing an interlocking geometry between the core and faceplates assists the adhesive bonding and ultimately strengthens the design. The top and bottom faceplate structures implement a sandwich design between the core cross members by means of paper honeycomb ribbed sections. The ribbed sections serve to provide stiffness at the spaced intervals between the core cross member extrusions.
- The composite structures within this work were produced by hand layup techniques. More advanced manufacturing processes can significantly increase the performance of the part and also further increase weight saving capabilities.
- Several options for optimizing the design of the *fiberplate* and *carbonplate* are available if needed. The comparison of the cross section core members revealed that the tube extrusion is not the most effective for loading applications and replacing this extrusion with a more beneficial design will also increase the performance. Optimization of the carbon fiber and fiberglass layups can also be performed to strengthen the laminate.

## FY 2005 PUBLICATIONS/PRESENTATIONS

1. Shoukry, S.N., G.W. William, J.C Prucz, R. Eluripati P. Shankaranarayana (2006). Multi-Fiber Unit Cell for Prediction of Residual Stresses in Continuous Fiber Composites. Accepted for publication at Mechanics of Advanced Materials and Structures.
2. Shoukry, S.N., J.C. Prucz, G. William, P. Shankaranarayana (2006). A parametric Study on Particulate Al-SiC Composite Bolted Joints. Proceedings of 2006 ASME International Mechanical Engineering Congress and Exposition, Chicago, Illinois USA, Paper No. IMECE2006-13253, November 2006.
3. Shoukry, S.N., J.C. Prucz, G. William (2006). A parametric Study on Particulate Al-SiC Composite Bolted Joints. Presented at the 43<sup>rd</sup> Annual Technical Meeting of the Society of Engineering Science, State College, Pennsylvania, August 2006.
4. Shoukry, S.N., J.C. Prucz, G. William (2006). Testing and 3D Finite Element Modeling of MMC Bolted Joints. *Proceedings of the 14<sup>th</sup> Annual International Conference on Composite/Nano Engineering*, Boulder, Colorado, USA, July 2006.
5. Shoukry, S.N., J.C. Prucz, G.W. William (2005). Multi-Fiber Unit cell for Prediction of Residual Stresses of Continuous Fiber Metal Matrix Composites. *Proceedings of the 12<sup>th</sup> Annual International Conference on Composite/Nano Engineering*, Tenerife, Canary Islands, Spain, July 2005.
6. Shoukry, S.N., G.W. William, J.C. Prucz, P. Shankaranaryana, and R. Eluripati (2005). Multi-Fiber Unit Cell for Prediction of Residual Stresses in Continuous Fiber Composites. *Proceedings of the 3rd International Conference on Structural Stability and Dynamics*, Kissimmee, Florida, June, 2005.

## THESES/DISSERTATIONS

1. Evans, Thomas H. (2006). Design of Composite Sandwich Panels for Lightweight Applications in Heavy Vehicle Systems. Master Thesis, Department of Mechanical and Aerospace Engineering, West Virginia University, Morgantown, WV.
2. Shankaranaryana, Praveen G. (2006). Microstructure Modeling and Finite Element Analysis of Particulate Reinforced Metal Matrix Composites. Master Thesis, Department of Mechanical and Aerospace Engineering, West Virginia University, Morgantown, WV.

## REFERENCES

- Bathe, K. J. (2002). ADINA Theory and Modeling Guide, Volume 1, ADINA R&D Inc., 71 Elton Ave., Watertown, MA 02472.
- Barbero, Ever J. (1998). *Introduction to Composite Material Design*, Edwards Brothers, Ann Arbor, MI, pp. 43-58.
- Chen, W.F. and D.J. Han (1987). *Plasticity for Structural Engineers*, Gau Liu Book Co., Taiwan.
- Hibbeler, R.C. (2005). *Mechanics of Materials*, 6<sup>th</sup> Edition, Pearson Prentice Hall, Upper Saddle River, NJ, 2005.
- Prucz, J.C. and S.N. Shoukry (2003). *Innovative Structural and Joining Concepts for Lightweight Design of Heavy Vehicle Systems*. 2003 Annual Progress Report on Heavy Vehicle Systems, U.S. Department of Energy, Washington, D.C.
- Prucz, J., S. Shoukry, G. William, T. Damiani, T. Evans, P. Shankaranarayana (2004). *Innovative Structural and Joining Concepts for Lightweight Design of Heavy Vehicle Systems*. 2004 Annual Progress Report on Heavy Vehicle Systems, U.S. Department of Energy, Washington, D.C., pp. 142-150.
- Prucz, J.C., Shoukry, S.N., G.W. William (2005). *Innovative Structural and Joining Concepts for Lightweight Design of Heavy Vehicle Systems*. Final Report No. EE50692 submitted to FreedomCAR and Vehicle Programs, US Department of Energy.
- Prucz, J., S. Shoukry, G. William, T. Damiani, T. Evans, P. Shankaranarayana (2005). *Innovative Structural and Joining Concepts for Lightweight Design of Heavy Vehicle Systems*. 2004 Annual Progress Report on Heavy Vehicle Systems, U.S. Department of Energy, Washington, D.C., pp. 142-150.